Atmospheric net particle accumulation on 96 plant species with contrasting morphological and anatomical leaf characteristics in a common garden experiment

Atmospheric net particle accumulation on 96 plant species with contrasting morphological and anatomical leaf characteristics in a common garden experiment

*S. Muhammad, K. Wuyts, R. Samson
Laboratory of Environmental and Urban Ecology, ENdEMIC research group, Department of Bioscience Engineering,
University of Antwerp, Groenenborgerlaan 171, 2020 Antwerp Belgium
samira.muhammad@uantwerpen.be, karen.wuyts@uantwerpen.be, roeland.samson@uantwerpen.be
*Corresponding author: samira.muhammad@uantwerpen.be
Tel: + 32 3 265 3569

ABSTRACT

Urban green spaces function as biological filters in reducing atmospheric particles. Yet there is a profound requisite to identify the most effective plant species by their leaf traits that can enhance particle capture and improve ambient air quality. In this study, we investigated leaves of 96 perennial urban plant species consisting of 43 deciduous broadleaf trees, 32 deciduous broadleaf shrubs, 14 deciduous and evergreen needle/scale-like, 5 evergreen broadleaves, and 2 climber species for their differences in net particle accumulation. Leaf saturation isothermal remanent magnetization (SIRM), a proxy for traffic and industry induced particle accumulation, along with morphological and anatomical leaf traits were analyzed in a common garden experiment in June and September 2016. Leaf SIRM varied significantly between plant species. The most effective net particle accumulating plant species with a median value of 23.0 µA were *Buddleja davidii*, *Viburnum opulus, Carpinus betulus*, *Quercus ilex, Viburnum lantana, Rosa rugosa, Sorbus aria, Aesculus hippocastanum*, *Pseudotsuga menziesii*, *Acer campestre*. The least effective net particle accumulating plant species with a median value of 10.4 µA were *Populus alba, Alnus glutinosa, Larix kaempferi, Larix decidua, Plantanus x acerilifolia, Acer pseudoplatanus, Robinia pseudoacacia, Quercus palustris, Rosa canina, Liquidambar styraciflua*. The “variable importance” in net particle accumulation for the investigated plant species was achieved using ®randomForest. The presence of leaf trichomes and specific leaf area were identified as important leaf traits for categorization of the selected plant species in low, medium, and high net particle accumulators. The extensive analysis of plant species at leaf-level with distinct micro-morphology contributes to a better understanding of plant species behavior in net particle capture and their contribution in reducing atmospheric particulate matter. Furthermore, this study has practical implications for policymakers in making informed choices when planning urban green infrastructures. Lastly, our study can become a basis to validate atmospheric deposition model using species-specific information.

KEYWORDS: Net particle accumulation, Particulate matter, Inter-species differences, Leaf traits, randomForest, Urban Environments

1. Introduction

Most air pollutants originate from human activities such as use of auto-motor vehicles, refineries, power plants, commonly known as an anthropogenic source (Bosko et al. 2005; Suzuki. 2006). Airborne particulate matter (PM) is the most problematic because of its adverse health effects (EEA, 2015). PM is segregated into different size fractions based on its aerodynamic diameter and expressed in µm. Particles ≤ 10 µm in aerodynamic diameter are classified as coarse particles or PM_{10}, those with an aerodynamic diameter of ≤ 2.5 µm are known as fine particles or $PM_{2.5}$ (WHO 2006). PM_{10} and $PM_{2.5}$ are inhalable particles which can penetrate the thoracic region of the respiratory system. In 2012, 432,000 premature deaths were attributed to elevated $PM_{2.5}$ concentrations in Europe of which approximately 403,000 deaths were in the European Union (EEA 2015). The foliage of plants permit entrapment of atmospheric PM, hence potentially improving the ambient air quality (McPherson et al. 2005; Nowak et al. 2006). Chen et al. (2017) suggest that leaves of higher plants due to their surface roughness and large contact area are likely to enhance the particle deposition.

Biomonitoring is the measurement of responses of living organisms that change in tandem with the environment (Nali and Lorenzini 2007). Magnetic biomonitoring, using magnetic properties of the biological material such as leaves and mosses, to assess ambient PM exposure is relatively fast and an inexpensive method (Hofman et al. 2017). The effect of leaf surface morphology on deposition velocities and differences in magnetic particle accumulation between species was observed by Mitchell et al. (2010) and Kardel et al. (2011) respectively. Most studies have applied magnetic biomonitoring to assess the temporal and intra-urban spatial variations in PM exposure (Kardel et al. 2012; Hofman et al. 2013; Barima et al. 2014). For a given PM source, saturation isothermal remanent magnetization (SIRM) and magnetic susceptibility of leaves relate significantly with ambient and accumulated atmospheric PM concentrations and leaf deposited PM mass (Hansard et al. 2011; Hofman et al. 2014). However, studies focusing on differences between plant species in leaf magnetic signals due to their different leaf surface micro-morphology and particle capturing abilities are few. The magnetic inter-species differences study, by Jordanova et al. (2010) reveals that lichens and mosses show the sharpest contrast between sites typically because lichens and mosses have greater lifespans in comparison to leaves of deciduous plant species (Innes 1985). Hence, they can be considered as long-term collectors. However, the limitation of lichens and mosses is that they are sensitive to anthropogenic pressures such as sulphur (S), nitrogen (N) deposition, drainage and managed burning (Van der Waal et al. 2011) which can make their distribution patchy and irregular in densely populated and industrial areas. Therefore, the effectiveness of higher plants in net particle accumulation is of relevance in urban environments where lichens are likely to be absent (Rai. 2013). Previous studies have indicated that plant species with broadleaves and rugged surface texture permit effective particle capture on their leaf surfaces compared to leaves with smooth surfaces (Beckett et al. 2000). However, evergreen needle-like surfaces were found to be more effective in particle accumulation than deciduous broadleaves (Beckett et al.1998; Sæbø et al. 2012) possibly because the latter may have a thicker boundary layer as hypothesized by Sæbø et al. (2012). Species-specific leaf traits such as leaf shape, trichome density of higher plants, which contribute towards net particle accumulation have been demonstrated (Kardel et al. 2012; Sæbø et al. 2012; Leonard et al. 2016) but rather qualitatively.

Due to the limited space in urban environments, the identification of effective plant species was of relevance. Moreover, the leaf traits which enhance particle capture needed to be identified. To date, most studies have identified differences in net particle accumulation at functional plant type level, i.e., deciduous broadleaves versus evergreen needle-like species comprising of a limited number of plant species (Beckett et al. 2000; Freer-Smith et al. 2004; Dzierzanowski et al. 2011; Grote et al. 2016). Besides, the leaf traits of investigated plant species were restricted to qualitative rather than quantitative measures (Beckett et al. 2000; Kardel et al. 2011; Mitchell et al. 2010).

Hence, the specific research aims of this study were to (I) determine the differences in net particle accumulation on the leaves of perennial urban plant species (n = 96) using magnetic analysis (II) identify the role of morphological and anatomical leaf traits in net particle accumulation using quantitative measures. In addition to magnetic analysis and easy-to-measure morphological and anatomical leaf traits, we will apply a ® randomForest (RF) algorithm, (III) where leaf traits of selected plant species (n = 96) will be ranked in the order of their importance in net particle accumulation abilities. We hypothesize that (a) net particle accumulation increases with leaf shape complexity and (b) greater trichome density, whereas it is (c) reduced with an increase in hydrophobicity of leaf surfaces.

2. Materials and methods

2.1 *Experimental setup and plant material*

The study was conducted as a common-garden experiment on the premises of the University of Antwerp (Antwerp, Belgium), i.e., in the 'Biogarden' site at Groenenborger campus. The site covered an area of 1200 m^2, and was located at 51º 10'46.0"N, 4º 25' 0.02"E. Ninety-six perennial plant species were selected to discern the differences in net particle accumulation. Selected plant species composed of varying leaf characteristics (i.e., size, shape, presence, and absence of trichomes, surface texture, i.e., smooth/glossy or rough /rugged. Forty-three deciduous broadleaf trees, thirty-two deciduous broadleaf shrubs, fourteen evergreen and deciduous needle/scale-like, five evergreen broadleaves, and two climber species were bought from one pesticide free nursery (Houtmeyers in Eindhout-Laakdal, Belgium 51º 6'6.22" N, 5º1'20.01"E) on the 22nd March 2016. For each species, five plants (replicates) were bought and placed in 15 L pots with organic potting soil (Peltracom NV, Belgium). The soil was infused with 150 g of Multicote 8, controlled release fertilizer (Haifa Group N: P: K of 15:7:15 with MgO and trace elements). All 480 plants were placed in pots by the 24th March 2016 and left to grow in the common-garden with a 1.5 m x 1.5 m arrangement. The spatial and atmospheric conditions were uniform for all plants. Regular watering of the plants was done to avoid drought stress. Moreover, the differences in soil characteristics were eliminated by using uniform potting soil. The plants were regularly monitored for any pests, disease or death due to stress. During the considered in leaf season (1st April – 30th September 2016) the mean $PM_{2.5}$ and PM_{10} concentration from the nearest air quality monitoring station (42R817, Antwerpen Groenenborgerlaan, at 250 m from the experiment site, operated by Flemish Environment Agency, VMM) were 11.2 and 21.8 µg/m^3 respectively (Fig.1). Meteorological data were obtained from the station Antwerpen Luchtbal (station 42M802, Havanastraat, operated by VMM). An average rainfall from April – September 2016 was recorded at 74.3 mm. An average air temperature of 15.4 ºC, wind speed of 3.1 m/s and relative air humidity of 72 % were recorded.

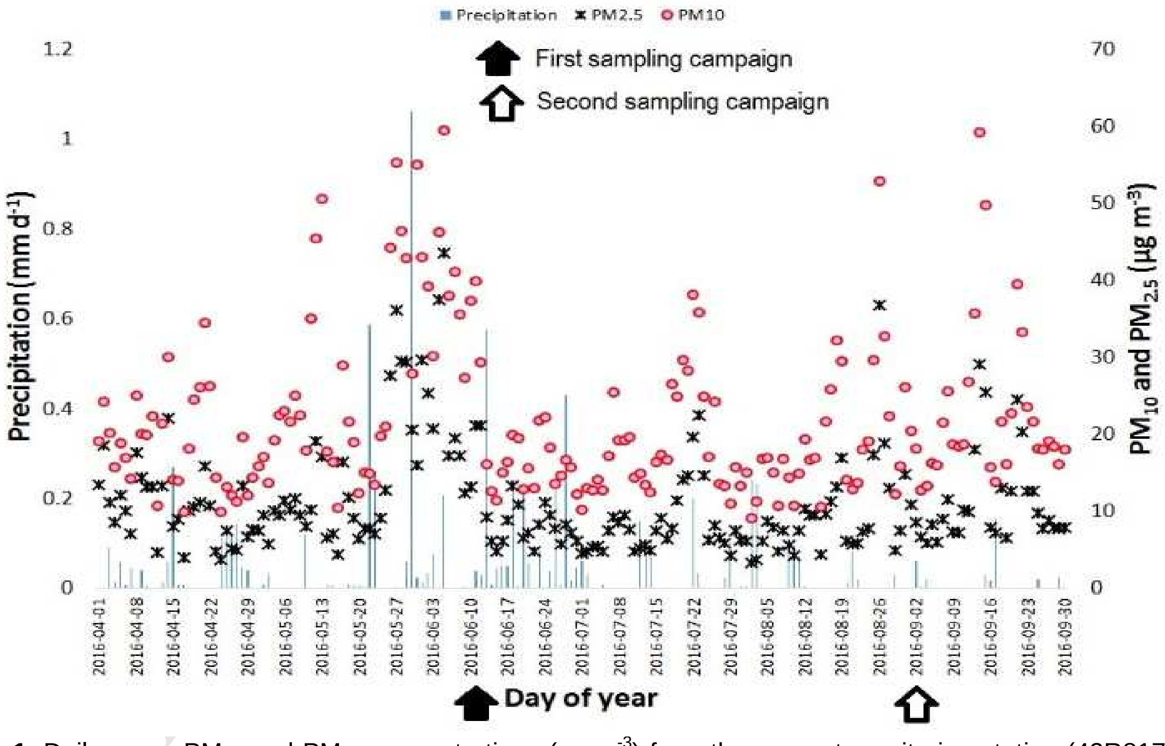

Fig. 1. Daily mean PM_{10} and $PM_{2.5}$ concentrations (µg m^{-3}) from the nearest monitoring station (42R817, Antwerpen, Groenenborgerlaan) and daily precipitation (mm d^{-1}) measured at Antwerpen Luchtbal (42M802 Havanstraat) illustrated from 1st April till 30th September 2016. First and second sampling campaign was organized on 9th to 10th June and 1st to 2nd September respectively. (Source: Flemish Environmental Agency, VMM).

2.2 *Leaf harvesting & sampling*

Leaf samples were collected twice during the growing season. The first sampling campaign was organized in June 2016 and the second in September 2016. No rain events occurred 3 - 5 days before or during either of the sampling campaigns. Mature undamaged leaves from the available replicates (n = 3 - 5) of investigated plant species were collected during two days to minimize variation due to differences in exposure time. For the June sampling campaign, the leaves of evergreen needle/scale-like, evergreen broadleaf, and climber plant species were about one year old while the leaves of deciduous plant species were from the current growing season. After harvesting, all leaves were stored in labeled paper envelopes and stored in a cool, dry facility until analyses. Only undamaged and non-infected leaves were used.

2.3 *Saturation isothermal remanent magnetization (SIRM)*

The leaf area of fresh leaves was measured using a leaf area meter (Li-3100, LiCor Biosciences). A leaf area of 100 - 150 cm^2 per replicate was maintained for magnetic analysis. After sampling, the leaves were stored in paper bags and oven dried at 50ºC for 5 – 7 days pending magnetic analysis. Before the determination of leaf saturation isothermal remanent magnetization (SIRM), we followed the preprocessing protocol of Hofman et al. (2013) where each sample was tightly packed in a cling film and pressed in a 7cm^3 plastic container. The sample containers were magnetized at a magnetic field of 1 T using a pulse magnetizer model 660 (2G Enterprises, Mountain View, California, USA). The remanent magnetic intensity was determined subsequently using a 2G magnetometer (2G Enterprises). For each measurement, the leaf sample container was placed at 'load position at 0º'. Next, samples were placed and measured at 'background-position' and finally at 'measurement position' to account for measurement variation. The magnetic moment measured in emu/cm^3 was multiplied by 10^{-3} to convert it to (Am^2). The resultant was divided by the area of the fresh leaf sample to obtain SIRM values normalized for the leaf surface area measured in (m^2). The final SIRM value is denoted as A (A = Am^2/m^2). All SIRM values reported in this study are expressed in µA. Magnetic measurements were carried out at the Royal Meteorological Institute of Belgium in Dourbes, Belgium.

2.4 *Leaf dissection index (LDI), roundness, and single leaf area (LA)*

Leaf shape complexity was determined using different leaf shape descriptors. Leaf samples from the June sampling campaign were measured for five leaf shape indicators, i.e., leaf dissection index (LDI) - the leaf perimeter was divided by square root of leaf area thus providing information on the complexity of leaf shape. A high leaf perimeter : leaf area ratio indicates a complex leaf shape (Nicotra et al. 2008), circularity (a function of leaf perimeter and leaf area), aspect ratio (maximum diameter divided by minimum diameter), roundness, and solidity (area of leaf divided by area of convex hull) (Russ 2002). An explanatory bi-plot of shape descriptors indicated that LDI was the inverse of circularity measurements whereas, the aspect ratio was the inverse of roundness. Therefore, we concluded to measure LDI and roundness (Russ 2002) for leaf samples from September sampling campaign. Roundness is similar to circularity measurements but is insensitive to irregular borders along the perimeter of an object. It considers the major axis of the best fit ellipse. The values range between 0 – 1. Three leaves from available replicates (n = 3 - 5) per plant species were scanned using a CanoScan LiDE 110 scanner (resolution of 300 dpi). The LDI (Eq.1) and roundness (Eq.2) were calculated as follows.

Eq.1 $$LDI = \frac{leaf\ perimeter}{\sqrt{leaf\ area}}$$

Eq.2 $$Roundness = 4 * \frac{leaf\ area}{\pi * (Major\ axis)^2}$$

The single leaf area (LA in cm^2) was measured for investigated plant species (n = 96) from available replicates (n = 3 - 5) using the same scanned images of leaves. The leaf area and perimeter measurements were obtained using ImageJ (https://imagej.nih.gov/ij/) in June and September.

2.5 *Leaf trichome density*

Trichome density (TD, the number of trichomes per leaf surface area), was obtained after following a chlorophyll clearing procedure. A single, mature, undamaged leaf from each plant species (n = 96) and available replicates (n = 3 - 5) was harvested in both June and September 2016. All leaves were observed under the binocular for the presence of trichomes, on both the abaxial and the adaxial leaf side. When trichomes were present, one small disc (approx. 12mm in diameter) per leaf was excised using a leaf perforator, from each replicate. Subsequently, following the chlorophyll clearing protocol of Gudesblat et al. (2012) and Pomeranz et al. (2013) the leaf discs were placed in 95 % ethanol (3 days) followed by 1.25 $_M$ NaOH: EtOH (1:1 v/v) solution for two hours, finally followed by 85 % lactic acid (3 – 5 days). The leaf discs were placed in multi-well plates to expedite the process and covered with a lid to avoid evaporation of the solution. Before mounting the discs on glass slides, all leaf discs were washed with 35 % ethanol. A drop of glycerin was placed on the slide, and with the help of tweezers, the cleared leaf discs were gently placed on a microscope slide and covered with a glass coverslip. The procedure was followed for both adaxial and abaxial leaf surfaces. All prepared slides were imaged using a light microscope (Olympus CX41) connected with a digital camera (Olympus UC30) along with an Olympus polarizing filter for high contrast images. Images obtained were imported in ImageJ software and analyzed using the cell counter plugin (Kurt De Vos). For each replicate and leaf side, ten images were analyzed. Therefore, approximately one hundred images per plant species were analyzed to calculate TD. An average count of trichomes in all replicates divided by the surface area of the images analyzed yielded the trichome density (mm^{-2}). Preliminary tests were conducted on a subset of plant species (n = 20) for temporal variation in TD from June to September; the paired sample t-test results [M = 1.75 ± 12.2, t (19) = 0.64, p = 0.530] did not show any significant differences in TD. Thus, TD for plant species (n = 51) was estimated once in September.

2.6 *Stomatal density (SD)*

Stomatal density (SD, the number of stomata per leaf surface area) was determined before the September field campaign. Imprints were taken on 29th and 30th August 2016 from both the abaxial and the adaxial leaf sides. The presence of dense trichomes hampered in obtaining good quality imprints. Hence, the stomatal imprints of leaves with dense trichomes were not included in the analysis and were procured from a subset of plant species (n = 38). A mature and undamaged leaf from each available replicate (n = 3 - 5) from the subset of plant species was harvested. Imprints were taken from the right side of the leaf on both the abaxial and the adaxial leaf surfaces. Following the protocol of (Kardel et al. 2010), a thin coat of colorless nail varnish was applied in an area between veins avoiding the midrib. After drying, the varnish film was gently removed using a transparent tape and affixed on to a microscope slide. The stomatal imprints were analyzed using a light microscope (Olympus CX41) connected with a digital camera (Olympus UC30) along with Olympus polarizing filter for high contrast images. Images obtained were analyzed using Cell-D software (Olympus) where the stomata were counted on a calibrated screen (mm^2) at a magnification of 4 x 10.

2.7 *Specific leaf area (SLA)*

Mature, undamaged leaves from available replicates (n = 3 - 5) of investigated plant species (n = 96) were collected in both June and September 2016. Leaf area measurements were conducted using leaf area meter (Li-3100, LiCor Biosciences). A leaf area of 100 - 150 cm^2 per replicate was maintained. Following the leaf area measurements, the samples were placed in labeled paper envelopes per species per replicate and oven dried at 50 ºC for 5 - 7 days. Subsequently, the dry leaf weight was determined using an electronic balance, (Denver, S-234) with an accuracy of 0.1 mg. Finally, the specific leaf area (SLA; expressed in m^2 kg^{-1}) was calculated as the leaf area (m^2) per unit leaf dry matter (kg^{-1}) (Larcher 2003). The same samples were used for leaf SIRM analyses (section 2.3).

2.8 *Leaf wettability*

Leaf wettability was determined by measuring the drop contact angle (DCA), the angle between a water droplet and the leaf surface (Holder 2012). Leaf wettability measurements were performed in both June and

September. For leaf wettability measurements, leaves were harvested separately and in batches on a span of ten days (13th – 24th June and 12th – 23rd September) after the main leaf harvesting campaign (section 2.2). Drop contact angle measurements were conducted on fresh leaf samples from available replicates (n = 3 - 5) of each plant species (n = 96) according to the method described by Kardel et al. (2012). Mature, undamaged leaves from each replicate were collected and placed in labeled paper bags. The DCA was obtained from both the abaxial (AB) and the adaxial (AD) leaf surface, avoiding the midrib and the leaf margin. The samples were affixed on wooden laths, using double-sided tape to procure a flat horizontal surface. At room temperature (21 °C) a 7.5 µL droplet of distilled water (for broadleaves) and 4 µL droplet (for needle/scale-like) was carefully placed on the sample using a micro-pipette. Next, using a Canon EOS 550D camera attached to a macro lens (MP-E 65mm 1:2.8) with 3x magnification, digital images of the droplets were acquired. The DCA images were taken within an hour of leaf harvesting. Finally, the left and the right contact angles were measured using ImageJ. The drop snake analysis plugin, where a polynomial fit is created around the droplet based on 10 – 12 manually placed points (Stalder et al. 2006) was used. The angle was measured between the perimeter of the droplet and the leaf surface. The DCA for a single replicate was calculated as an average of left and right angle. Whereas, the DCA for a plant species was calculated as an average of all replicates.

2.9. *Data analysis*

A multiple linear regression (MLR) was applied to identify the relationship between leaf traits of the selected plant species (n = 96) and net particle accumulation, with leaf SIRM as the dependent variable. The MLR was first applied on the June data consisting of only deciduous needle-like, deciduous broadleaf tree and shrub species (n = 77). Second, the MLR was applied on the September data for all selected plant species (n = 96). The leaves of evergreen needle/scale-like, evergreen broadleaves, and climber plant species were excluded from the analysis in June because the leaves of these plant species were about one-year-old in June. In September, the response variable (leaf SIRM) for investigated deciduous plant species (n = 77) was adjusted for equal exposure time by subtracting the June leaf SIRM from September leaf SIRM. The leaf SIRM of evergreen needle/scale-like, evergreen broadleaves and climber species, was set to September leaf SIRM assuming the June leaf SIRM to be zero. As such the net particle accumulation abilities of the investigated plant species could be fairly compared as exposure times were set equal. The examined plant species were grouped into three classes of (low, medium, high) using quantile classification for their effectiveness in net particle accumulation. The MLR was initialized with all explanatory variables (Eq.3): LDI, leaf roundness, SD, TD, LA, SLA and DCA (AB, AD) and successively reduced to the most significant contributing variables based on the comparison of models with the Akaike Information Criterion (AIC). The response variable leaf SIRM was transformed using natural log (ln). Normality of residuals was checked by Shapiro-Wilk test, normal probability plots and plots of residual values versus fitted values.

Eq.3

$$y_i = \beta_0 + \beta_1 LDI_i + \beta_2 leafroundness_i + \beta_{3SD_i} + \beta_4 TD_i + \beta_5 LA_i + \beta_6 SLA_i + \beta_7 DCA(AB)_i + \beta_8 DCA(AD)_i + \epsilon_i$$

Where y_i is the response variable (leaf SIRM), β_0 is the intercept, β_{1-8} are partial regression coefficients, LDI_i, $leafroundness_i$, SD_i, TD_i, LA_i, $DCA(AB)_i$, $DCA(AD)_i$ are the predictor variables and ϵ_i is the random error.

Principal component analysis (PCA) was applied to LDI, leaf roundness, SD, TD, LA, SLA, and DCA (AB, AD) to distinguish the explanatory variables and identify clusters in observations. A dendrogram using the Ward algorithm (ward.D2) was constructed to procure a cluster of plant species. Leaves of plant species that were morphologically and anatomically analogous to each other were clustered into a group. To identify the differences in leaf SIRM between clusters (n = 5), families (n = 29) and functional plant types (n = 5), one-way analysis of variance (ANOVA) was performed. Post-hoc multiple comparison analysis tests were performed with Tukey's honest significant difference (Tukey-HSD) method. We applied ® randomForest (RF), a machine learning method to rank input variables on the basis of their importance (Breiman 2001; Philibert et al. 2013). The primary principal of RF is to combine numerous binary decision trees using several bootstrap samples coming from the learning sample. About one-third of the initial number of observations are not selected and referred to as out-of-bag (OOB) data. At each node, a subset of explanatory variables denoted as ***mtry*** are randomly selected (Breiman 2001). The number of decision trees used to build the model are denoted as ***ntree***. A measure to rank the predictors/explanatory variables on the basis of their importance is known as variable importance (VI). Breiman (2001) recommend that variable importance should be done using the mean decrease accuracy (MDA). Because it is the normalized difference of the classification accuracy for the OOB data (Cutler et al. 2007). A higher MDA indicates variables that are of most importance to the classification. In RF the misclassification error rate is estimated using the OOB data and termed as OOB error rate (Breiman, 2001). The parameters *mtry* and *ntree* were set to 4 and 500 respectively. The "depend" variable, leaf SIRM was grouped into three classes using quantile classification. A separate RF model was built for each of the nine data subsets as described in (Table 1). It is important to note that VI was specific to each RF model. All statistical testing was done using R 3.2.2 software (R Core Team 2015), the *Stats* package (R Core Team and contributors worldwide) the party package (Hothorn et al. 2006) and the ® randomForest package (Liaw and Wiener, 2002).

Table 1

Overview of the data subsets used for ® randomForest (RF) built according to the functional plant types and time period considered. N = number of plant species included. Observations = number of observations included in the RF model. Model "AS" - all plant species (n = 96) in September. "BJ" – deciduous needle-like and broadleaves for June. "BS"- deciduous needle-like and broadleaves for September. "BD" Difference (∆) in leaf SIRM between June and September for deciduous needle-like and broadleaves. "EJ"- evergreen: needle/scale-like, broadleaves, and climber species for June. "ES"- evergreen: needle/scale-like, broadleaves, and climber species for September. "AS-SD"- plant species accounted for stomatal density in September. "DEBS-TD" deciduous and evergreen broadleaf plant species with trichome density in September. "DEBD-TD" – deciduous and evergreen broadleaf plant species with trichome density with the difference in leaf SIRM between June and September.

Model	Type	Time period	N	Observations
AS	All species	September	96	466
BJ	Deciduous needle-like and broadleaves	June	77	364
BS	Deciduous needle-like and broadleaves	September	77	364
BD	Deciduous needle-like and broadleaves	∆ June – September	77	364
EJ	Evergreen (needle-like/ broadleaves)	June	19	98
ES	Evergreen (needle-like/ broadleaves)	September	19	103
AS-SD	All species with SD data	September	38	187
DEBS-TD	All broadleaves with TD data	September	51	247
DEBD-TD	All broadleaves with TD data	∆ June – September	51	247

3. Results

3.1 *Leaf SIRM and differences between plant species, families and types*

The leaf SIRM values varied between plant species and throughout the growing season (Table 2, Fig. 2). In June, the leaf SIRM of deciduous: needle-like, broadleaf tree and shrub species (n = 77) ranged between 1.3 – 15.7 µA with the lowest leaf SIRM observed on leaves of *Salix purpurea* and highest on leaves of *Viburnum lantana.* In September, considering the equal exposure time, the leaf SIRM of all investigated plant species (n = 96) ranged from 0.7 – 31.6 µA with the lowest and highest leaf SIRM on leaves of *Populus alba* and *Buddleja davidii* respectively.

In June, the median leaf SIRM of deciduous: needle-like, broadleaf tree and shrub species (n = 77) by family ranged between 2.1 – 7.6 µA. The lowest median leaf SIRM was observed for the family Fabaceae (n = 2) and the highest for Elaeagnaceae (n = 2). In September, the median leaf SIRM by family consisting of all plant species (n = 96) ranged between 2.1 – 31.6 µA. The lowest leaf SIRM was observed for the family Platanaceae (n = 1) and highest for the family Scrophulariaceae (n = 1).

In June, one-way analysis of variance (ANOVA) between functional plant types, i.e., deciduous broadleaf trees and deciduous broadleaf shrubs showed no significant difference in leaf SIRM ($p > 0.05$). The median leaf SIRM values for deciduous broadleaf trees and deciduous broadleaf shrubs were 5.3 µA and 5.0 µA respectively. The paired sample t-test conducted on leaf SIRM of deciduous broadleaf trees and deciduous broadleaf shrubs between June and September showed a significant increase ($p < 0.001$) in September (Fig. 3a). With an equal exposure time for all plant types (n = 5), ANOVA showed these differences between functional plant types were not significant ($p > 0.05$) (Fig. 3b). The median leaf SIRM values for deciduous broadleaf trees, deciduous broadleaf shrubs, evergreen broadleaves, needle/scale-like and climber species were 9.7, 12.1, 12.4, 12.0, and 9.5 µA respectively.

ACCEPTED MANUSCRIPT

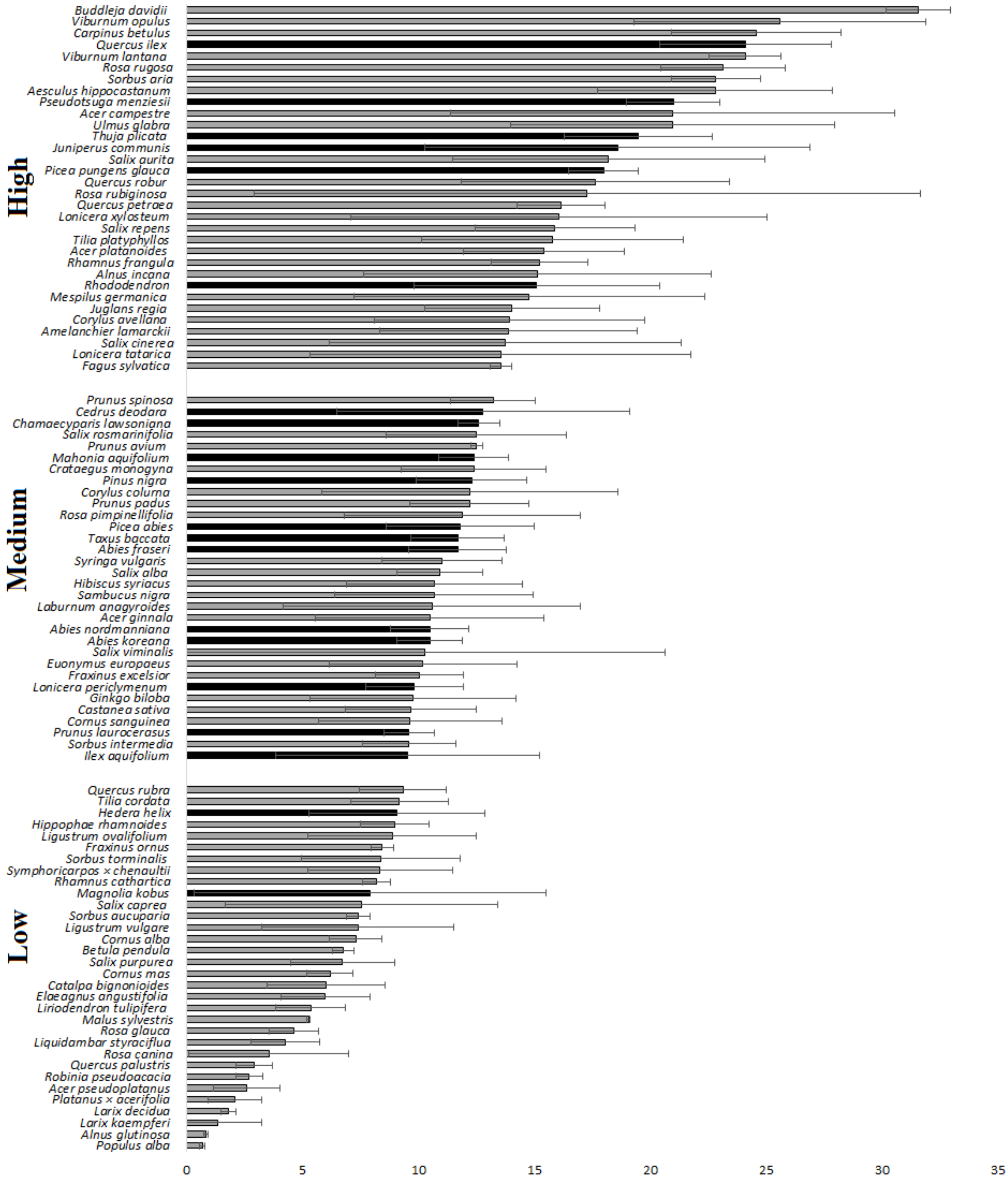

Fig. 2. Mean leaf area-normalized SIRM (µA) of selected urban plant species (n = 96) from a common garden in September 2016. Error bars are standard deviations. Gray bars – deciduous: needle-like, broadleaf tree and shrub species, Black bars – evergreen: needle/scale-like, broadleaf and climber species. Note: Leaves of evergreen: needle/scale-like, broadleaf and climber species sampled in June were developed in the previous growing season and were about one year old in June. The leaf SIRM for investigated deciduous needle-like, broadleaf tree and shrub species (n = 77) were adjusted for equal exposure time by subtracting the June leaf SIRM from September leaf SIRM. The leaf SIRM of needle/scale-like, evergreen broadleaves and climber species, was set to September leaf SIRM assuming the June leaf SIRM to be zero. Plant species grouped according to leaf SIRM into (low, medium, high) class using quantile classification.

Table 2

Analyzed plant species (n = 96) with indication of family (n = 29) denoted as (1 - 29) # see text box below and plant type (n = 5, C = conifer, E.B = evergreen broadleaf, T = deciduous tree, S = deciduous shrub, CL = climber) with clusters (n = 5) based on morphological and anatomical leaf traits– Single leaf area (LA cm^2) specific leaf area (SLA m^2 kg^{-}1), leaf dissection index (LDI dimensionless), leaf roundness (dimensionless) drop contact angle (DCA °) at abaxial (AB) and adaxial (AD) leaf side Saturation Isothermal Remanent Magnetization (SIRM µA). Stomatal density (mm^{-2}) and trichome density (mm^{-2}), trichome presence "N" = No, "Y" = Yes, "+++" dense fibrous network of trichomes - trichome density not measured, "n/a" trichomes present but not captured in the sample due to sparse presence. Leaves of plant species names in the bold text are one year old in June 2016 and have missing leaf SIRM values indicated by a hyphen "-".

		JUNE							SEPTEMBER									
Plant species	Cluster	LA	SLA	LDI	Leaf roundness	DCA (AB)	DCA (AD)	SIRM	LA	SLA	LDI	Leaf roundness	DCA (AB)	DCA (AD)	SIRM	Stomatal density	Trichome presence	Trichome density
Abies fraseri **(C)** [21]	3	0.26	3.34	16.54	0.12	73	72	-	0.10	6.00	12.77	0.09	90	56	11.68	122.4	N	0.00
Abies koreana **(C)** [21]	3	0.28	3.31	15.20	0.14	115	89	-	0.36	5.88	12.65	0.14	111	66	10.49	131.5	N	0.00
Abies nordmanniana **(C)** [21]	3	0.45	3.31	16.99	0.10	72	68	-	0.45	5.34	15.99	0.10	64	64	10.28	104.2	N	0.00
Acer campestre (T) [26]	4	27.14	14.79	11.52	0.86	69	83	7.91	28.04	13.39	14.09	0.90	67	78	28.88	0.0	Y	4.04
Acer ginnala (T) [26]	2	30.52	18.31	10.67	0.83	88	81	3.99	28.35	13.70	9.99	0.78	61	73	14.47	628.1	N	0.00
Acer platanoides (T) [26]	4	87.05	19.70	13.43	0.85	86	96	5.58	71.82	14.28	13.97	0.78	76	67	20.96	0.0	Y	n/a
Acer pseudoplatanus (T) [26]	5	113.28	15.98	11.87	0.78	133	76	6.46	96.95	13.39	15.22	0.94	106	63	9.07	0.0	N	0.00
Aesculus hippocastanum (T) [26]	4	85.52	13.15	8.89	0.47	97	84	6.80	65.01	9.91	9.36	0.45	88	62	29.59	0.0	Y	9.96
Alnus glutinosa (T) [6]	4	43.62	16.42	7.59	0.90	65	65	8.15	48.59	18.85	7.40	0.82	59	58	9.00	0.0	Y	0.46
Alnus incana (T) [6]	5	38.84	19.48	7.90	0.83	115	75	5.27	50.26	13.76	7.81	0.79	98	69	20.43	0.0	Y	9.00
Amelanchier lamarckii (S) [24]	2	22.70	18.54	8.04	0.57	113	85	3.71	24.50	13.49	8.12	0.65	77	85	17.55	97.9	N	0.00
Betula pendula (T) [6]	4	14.71	22.20	9.63	0.79	73	75	3.53	22.17	14.48	9.89	0.89	76	74	10.35	0.0	Y	n/a
Buddleja davidii (S) [27]	1	33.46	12.17	11.84	0.49	133	76	6.41	32.49	10.29	8.80	0.47	124	63	37.97	0.0	Y	+++
Carpinus betulus (T) [6]	4	14.85	18.54	8.74	0.57	89	76	6.32	25.16	14.22	8.71	0.62	67	74	30.95	0.0	Y	1.17
Castanea sativa (T) [15]	4	65.12	16.55	10.88	0.35	68	73	6.02	68.04	10.99	12.36	0.31	64	70	15.72	0.0	Y	13.58
Catalpa bignonioides (T) [7]	2	64.77	25.43	7.52	0.73	94	79	3.70	171.89	16.37	8.00	0.87	80	62	9.73	422.1	Y	5.29
Cedrus deodara **(C)** [21]	3	0.64	2.42	25.99	0.03	96	101	-	0.18	3.83	26.40	0.05	71	79	12.77	155.3	N	0.00
Chamaecyparis lawsoniana **(C)** [11]	3	27.86	4.58	41.85	0.46	111	117	-	61.09	8.04	42.50	0.56	108	104	12.59	0.0	N	0.00
Cornus alba (S) [10]	5	38.69	22.13	7.28	0.55	120	88	3.80	50.80	17.23	7.93	0.63	111	73	11.13	0.0	Y	21.54
Cornus mas (T) [10]	4	21.60	15.36	7.15	0.64	78	83	4.86	25.01	10.38	7.67	0.64	62	74	11.00	0.0	Y	5.96
Cornus sanguinea (S) [10]	4	30.14	19.15	7.09	0.85	81	74	3.16	43.94	13.29	8.03	0.78	63	74	12.84	0.0	Y	15.63
Corylus avellana (S) [6]	4	61.17	17.34	8.98	0.87	77	76	6.37	77.53	16.05	9.47	0.84	63	69	20.27	0.0	Y	4.38
Corylus colurna (T) [6]	4	20.65	20.70	9.28	0.81	62	56	8.18	72.90	15.48	8.29	0.91	57	63	20.43	0.0	Y	9.50
Crataegus monogyna (T) [24]	4	14.07	17.12	10.97	0.92	98	78	3.81	12.34	10.62	13.20	0.95	72	65	16.15	0.0	Y	1.08
Elaeagnus angustifolia (T) [12]	5	7.28	18.35	8.13	0.30	147	85	8.11	10.13	20.16	7.93	0.42	124	79	14.12	0.0	Y	45.13
Euonymus europaeus (S) [9]	4	18.65	14.63	7.97	0.53	88	88	4.99	27.16	13.22	7.96	0.60	63	74	15.24	0.0	Y	n/a
Fagus sylvatica (T) [15]	4	12.59	19.00	7.18	0.62	92	90	8.55	11.78	17.27	7.37	0.60	69	75	22.07	0.0	Y	9.67
Fraxinus excelsior (T) [20]	4	14.25	15.90	8.31	0.48	71	80	4.34	23.23	12.94	9.47	0.46	55	64	14.44	0.0	Y	n/a

Plant species	Cluster	JUNE LA	JUNE SLA	JUNE LDI	JUNE Leaf roundness	JUNE DCA (AB)	JUNE DCA (AD)	JUNE SIRM	SEPTEMBER LA	SEPTEMBER SLA	SEPTEMBER LDI	SEPTEMBER Leaf roundness	SEPTEMBER DCA (AB)	SEPTEMBER DCA (AD)	SEPTEMBER SIRM	Stomatal density	Trichome presence	Trichome density
Fraxinus ornus (T) [20]	2	15.88	16.16	8.27	0.48	80	67	4.05	14.17	11.90	9.73	0.57	67	67	12.46	222.9	N	0.00
Ginkgo biloba (T) [16]	5	22.78	11.77	9.80	0.74	131	127	3.14	27.41	8.75	10.83	0.66	117	70	12.89	56.9	N	0.00
***Hedera helix* (CL)** [3]	4	30.79	11.60	6.99	0.80	74	82	-	23.38	11.71	7.87	0.80	72	74	9.09	0.0	Y	0.58
Hibiscus syriacus (S) [19]	2	15.38	22.33	8.18	0.76	77	73	3.90	21.03	15.18	9.49	0.66	60	62	14.60	342.9	Y	1.29
Hippophae rhamnoides (S) [12]	5	2.26	11.87	11.89	0.12	117	86	7.11	2.75	11.80	13.47	0.12	101	84	16.11	0.0	N	0.00
***Ilex aquifolium* (E.B)** [4]	2	13.13	6.98	12.31	0.41	93	89	-	15.98	6.53	12.33	0.53	80	83	9.54	192.9	N	0.00
Juglans regia (T) [17]	2	49.52	19.74	7.52	0.53	76	71	3.26	56.72	12.31	7.58	0.57	60	69	17.33	220.1	N	0.00
***Juniperus communis* (C)** [11]	3	0.20	3.50	13.45	0.11	99	89	-	0.19	4.69	15.06	0.10	81	72	18.59	19.2	N	0.00
Laburnum anagyroides (T) [14]	5	12.50	15.57	8.26	0.48	133	113	2.41	16.83	14.47	8.10	0.48	115	76	13.02	0.0	Y	11.13
Larix decidua (T) [21]	3	0.22	8.29	19.11	0.07	114	105	6.58	0.29	8.71	22.41	0.08	84	76	8.39	150.7	N	0.00
Larix kaempferi (T) [21]	3	0.19	6.00	17.57	0.07	111	112	5.95	0.54	10.39	25.79	0.11	101	87	7.29	0.0	N	0.00
Ligustrum ovalifolium (S) [20]	2	9.98	11.56	7.64	0.54	85	79	4.52	21.14	9.50	7.95	0.48	60	71	13.37	417.0	N	0.00
Ligustrum vulgare (S) [20]	2	5.35	13.95	7.86	0.36	95	98	5.51	11.46	10.17	8.23	0.34	85	74	12.94	203.3	N	0.00
Liquidambar styraciflua (T) [2]	2	20.31	21.54	10.30	0.86	98	98	3.61	46.60	15.29	14.16	0.92	83	67	7.88	183.5	N	0.00
Liriodendron tulipifera (T) [18]	5	54.62	24.06	9.22	0.88	135	133	2.44	182.28	21.97	11.62	0.82	125	93	7.80	166.7	N	0.00
***Lonicera periclymenum* (CL)** [8]	5	15.14	19.21	7.06	0.70	134	123	-	23.77	16.67	7.38	0.74	105	93	9.83	212.0	Y	3.92
Lonicera tatarica (S) [8]	5	10.65	14.32	6.89	0.74	137	136	3.74	11.62	10.39	6.80	0.82	112	58	17.30	156.8	N	0.00
Lonicera xylosteum (S) [8]	5	14.32	18.30	7.06	0.68	140	134	3.62	18.92	13.86	7.00	0.60	112	69	19.70	0.0	Y	8.83
Magnolia kobus (T) [20]	2	41.89	20.82	7.77	0.44	101	104	4.89	48.09	18.56	8.76	0.48	77	64	12.83	226.8	Y	5.75
***Mahonia aquifolium* (E.B)** [5]	2	9.93	14.31	7.77	0.50	132	86	-	21.99	9.38	8.30	0.59	89	69	12.42	302.1	N	0.00
Malus sylvestris (T) [24]	1	24.04	18.34	8.25	0.56	93	81	7.33	29.54	14.02	9.00	0.69	87	76	12.62	0.0	Y	+++
Mespilus germanica (T) [24]	4	22.15	14.96	7.80	0.48	92	85	7.91	18.58	10.21	8.15	0.47	71	74	22.70	0.0	Y	21.33
***Picea abies* (C)** [21]	3	0.19	4.01	19.39	0.07	100	104	-	0.20	5.64	18.46	0.09	66	82	11.78	187.9	N	0.00
***Picea pungens glauca* (C)** [21]	3	0.26	3.44	16.24	0.10	80	82	-	0.30	3.84	16.87	0.09	88	93	17.97	183.3	N	0.00
***Pinus nigra* (C)** [21]	3	1.30	6.62	29.09	0.09	76	86	-	1.10	4.61	33.02	0.05	75	77	12.30	168.1	N	0.00
Platanus × acerifolia (T) [22]	4	101.59	21.20	9.18	0.85	99	83	4.92	90.00	16.66	12.05	0.84	55	80	7.01	0.0	Y	2.08
Populus alba (T) [25]	4	53.48	19.78	8.79	0.83	93	85	2.40	61.48	20.64	8.39	0.81	75	76	3.08	0.0	Y	n/a
Prunus avium (T) [24]	2	40.36	21.67	8.37	0.56	87	86	5.39	40.97	14.50	8.90	0.57	74	64	17.88	348.6	Y	3.17
***Prunus laurocerasus* (E.B)** [24]	2	38.30	9.90	7.57	0.52	85	85	-	48.46	7.83	10.05	0.49	81	78	9.60	179.3	N	0.00
Prunus padus (S) [24]	5	30.62	15.59	8.34	0.53	126	92	5.89	53.22	11.21	8.52	0.53	96	69	18.15	0.0	Y	0.13
Prunus spinosa (S) [24]	4	7.02	13.86	7.05	0.63	100	86	7.07	10.96	9.92	7.98	0.60	82	66	20.33	0.0	Y	8.17
***Pseudotsuga menziesii* (C)** [21]	3	0.34	5.29	18.2	0.08	90	84	-	0.15	6.63	18.34	0.05	91	76	21.05	143.8	N	0.00
***Quercus ilex* (E.B)** [15]	1	19.55	8.52	7.64	0.56	130	71	-	10.07	6.83	8.06	0.49	100	66	24.08	0.0	Y	+++
Quercus palustris (T) [15]	2	26.80	17.53	13.7	0.38	99	87	5.56	23.91	16.98	14.52	0.41	57	65	8.48	428.8	N	0.00
Quercus petraea (T) [15]	2	16.29	14.24	9.79	0.58	133	93	5.93	27.07	12.39	10.62	0.48	110	75	22.10	551.0	Y	13.38

Plant species	Cluster	JUNE LA	JUNE SLA	JUNE LDI	JUNE Leaf roundness	JUNE DCA (AB)	JUNE DCA (AD)	JUNE SIRM	SEPTEMBER LA	SEPTEMBER SLA	SEPTEMBER LDI	SEPTEMBER Leaf roundness	SEPTEMBER DCA (AB)	SEPTEMBER DCA (AD)	SEPTEMBER SIRM	Stomatal density	Trichome presence	Trichome density
Quercus robur (T) [15]	2	19.02	16.94	12.55	0.49	131	119	4.26	25.32	13.08	11.73	0.54	94	80	21.89	446.7	N	0.00
Quercus rubra (T) [15]	5	62.57	15.95	12.29	0.61	122	104	5.36	59.32	12.48	13.14	0.45	76	75	14.67	0.0	Y	n/a
Rhamnus cathartica (S) [23]	2	11.85	17.63	8.02	0.57	84	68	8.41	27.21	12.60	7.81	0.62	76	68	16.60	236.5	Y	1.17
Rhamnus frangula (S) [23]	2	15.58	21.31	7.25	0.63	91	83	4.98	19.26	16.15	7.79	0.57	62	71	20.16	406.2	N	0.00
***Rhododendron* (E.B)** [13]	2	27.68	10.16	8.08	0.35	58	76	-	46.74	6.48	8.63	0.35	55	59	15.06	255.5	N	0.00
Robinia pseudoacacia (T) [14]	5	8.24	28.26	7.18	0.70	141	132	1.71	10.50	23.59	7.31	0.49	125	123	4.41	0.0	Y	31.79
Rosa canina (S) [24]	2	4.74	16.82	7.97	0.67	97	123	5.66	4.46	14.44	9.29	0.62	89	103	9.22	131.8	N	0.00
Rosa glauca (S) [24]	5	5.87	17.92	8.78	0.67	131	129	3.14	6.39	13.89	8.13	0.53	126	124	7.77	84.0	N	0.00
Rosa pimpinellifolia (S) [24]	5	1.93	19.45	7.81	0.63	128	128	5.00	2.60	11.74	8.68	0.58	90	80	16.91	0.0	Y	n/a
Rosa rubiginosa (S) [24]	4	4.85	15.73	7.55	0.75	69	89	7.31	4.82	10.74	7.83	0.72	59	66	24.61	0.0	Y	9.88
Rosa rugosa (S) [24]	5	8.07	17.29	7.64	0.67	124	81	5.76	10.59	8.33	7.39	0.57	100	58	28.90	0.0	Y	28.88
Salix alba (T) [25]	5	9.42	17.40	8.93	0.27	125	74	3.78	17.01	11.89	11.12	0.26	110	67	14.68	0.0	Y	19.83
Salix aurita (S) [25]	5	5.48	20.44	7.50	0.75	134	120	4.60	9.64	14.38	7.51	0.68	126	68	22.80	0.0	Y	16.21
Salix caprea (T) [25]	5	19.09	22.42	7.67	0.67	133	71	4.74	36.82	16.34	8.00	0.74	125	64	12.27	0.0	Y	11.13
Salix cinerea (S) [25]	5	11.31	22.76	8.05	0.42	130	85	4.95	20.48	16.44	8.80	0.34	124	83	18.72	0.0	Y	20.46
Salix purpurea (S) [25]	2	4.86	19.69	9.13	0.35	130	132	1.34	12.05	14.72	11.31	0.19	121	112	8.07	735.9	N	0.00
Salix repens (S) [25]	5	1.59	14.89	7.31	0.47	129	69	6.00	4.62	12.31	7.67	0.55	123	81	21.89	0.0	Y	38.42
Salix rosmarinifolia (S) [25]	1	3.81	13.89	16.46	0.08	137	69	5.18	4.96	9.89	15.84	0.08	128	78	17.71	0.0	Y	+++
Salix viminalis (S) [25]	5	17.83	18.49	11.45	0.16	130	85	5.53	15.60	18.90	11.58	0.14	128	84	15.78	0.0	Y	16.96
Sambucus nigra (S) [1]	4	30.66	18.22	9.70	0.50	56	64	4.92	33.66	17.70	10.77	0.52	54	64	15.58	0.0	Y	1.38
Sorbus aria (T) [24]	1	25.12	16.53	9.12	0.75	139	82	7.36	43.12	11.37	9.26	0.64	130	61	30.21	0.0	Y	+++
Sorbus aucuparia (T) [24]	5	5.38	15.49	10.46	0.33	131	78	10.13	8.88	12.03	10.36	0.31	86	75	17.47	0.0	Y	3.29
Sorbus intermedia (T) [24]	1	30.87	11.10	10.37	0.55	135	79	13.87	40.89	7.87	12.08	0.53	110	63	23.53	0.0	Y	+++
Sorbus torminalis (T) [24]	4	50.64	13.09	11.76	0.83	84	77	5.12	40.43	11.23	11.52	0.80	61	59	13.49	0.0	Y	10.46
Symphoricarpos × chenaultii (S) [8]	5	3.11	13.59	7.14	0.62	140	135	4.34	2.90	13.72	7.27	0.72	126	92	12.70	0.0	Y	19.46
Syringa vulgaris (S) [20]	4	30.48	9.02	7.30	0.69	56	79	4.59	39.06	8.63	7.72	0.65	56	63	15.59	0.0	N	0.00
***Taxus baccata* (C)** [28]	2	0.46	7.10	10.93	0.13	94	75	-	0.46	6.78	11.88	0.12	86	66	11.69	94.5	N	0.00
***Thuja plicata* (C)** [11]	3	58.58	4.83	26.95	0.65	104	83	-	30.65	5.24	38.04	0.42	93	64	19.54	0.0	N	0.00
Tilia cordata (T) [19]	4	30.22	22.83	9.38	0.92	74	66	3.61	49.88	15.70	7.60	0.89	70	76	12.76	0.0	N	0.00
Tilia platyphyllos (T) [24]	4	38.78	23.31	8.21	0.85	84	59	5.61	82.97	15.11	8.71	0.88	61	59	21.39	0.0	Y	6.75
Ulmus glabra (T) [29]	4	34.43	17.19	8.87	0.66	85	85	6.12	68.01	12.28	9.52	0.87	67	55	27.06	0.0	Y	10.29
Viburnum lantana (S) [1]	4	36.77	12.86	7.39	0.80	79	76	15.74	40.78	10.07	7.75	0.69	58	71	39.77	0.0	Y	8.38
Viburnum opulus (S) [1]	4	37.42	17.88	11.57	0.89	95	74	5.40	59.53	11.65	9.87	0.87	77	71	31.01	0.0	Y	22.29

 # Plant families: 1 = Adoxaceae 2 = Altingiaceae 3 = Apiaceae 4 = Aquifoliaceae

5 = Berberidaceae	6 = Betulaceae	7 = Bignoniaceae	8 = Caprifoliaceae	9 = Celastreaceae
10 = Cornaceae	11 = Cupressaceae	12 = Elaeagnaceae	13 = Ericaceae	14 = Fabaceae
15 = Fagaceae	16 = Ginkgoaceae	17 = Juglandaceae	18 = Magnoliaceae	19 = Malvaceae
20 = Oleaceae	21 = Pinaceae	22 = Platanaceae	23 = Rhamnaceae	24 = Rosaceae
25 = Salicaceae	26 = Sapindaceae	27 = Scrophulariaceae	28 = Taxaceae	29 = Ulmaceae

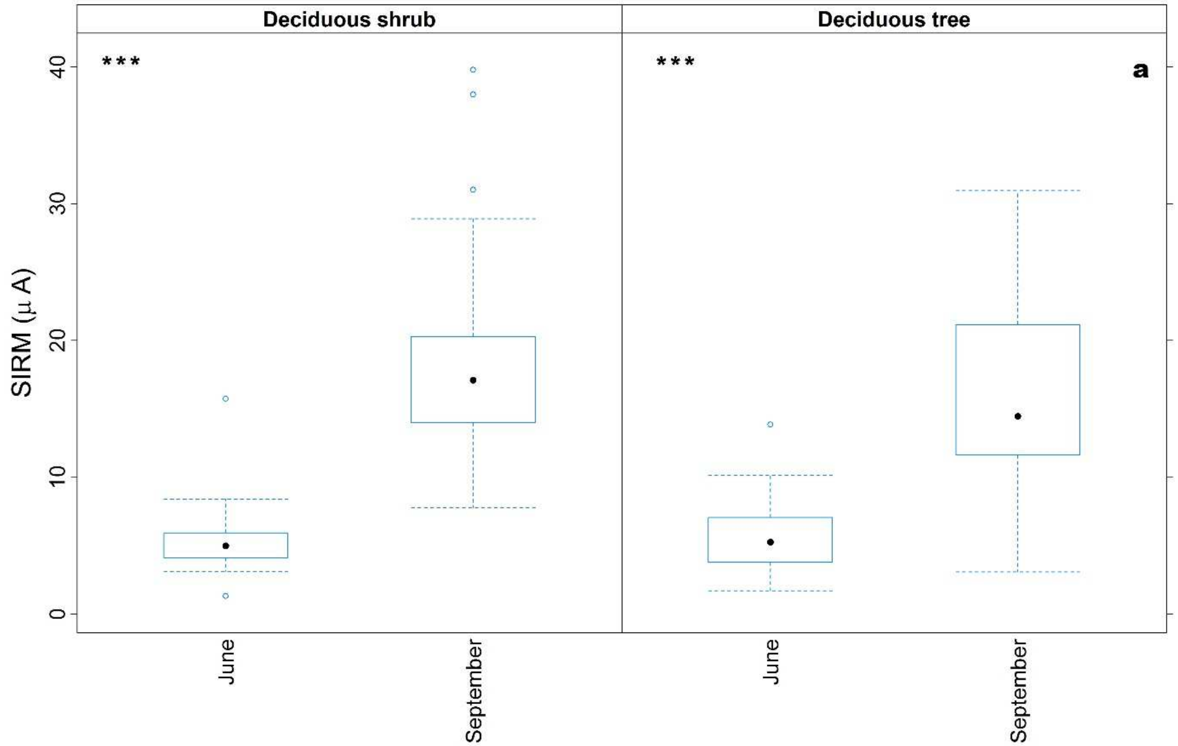

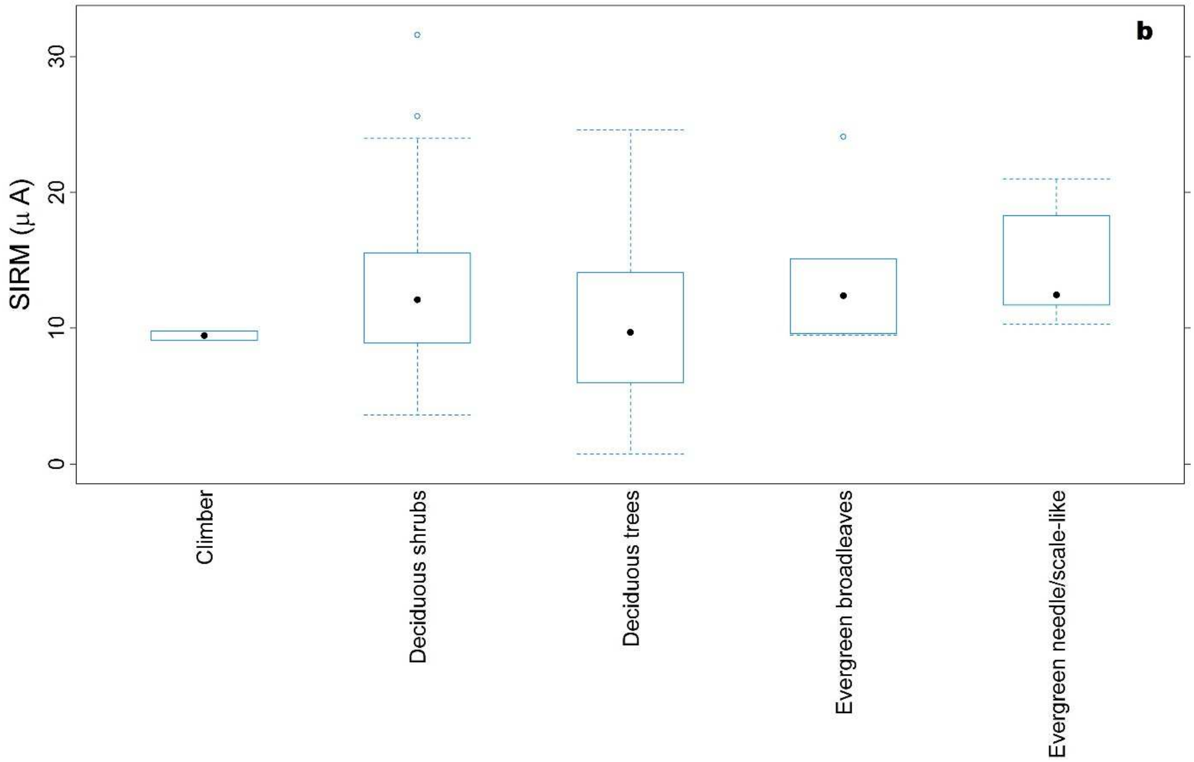

Fig. 3. (a) Box plots for leaf SIRM of deciduous needle-like and broadleaf trees (n = 45) and deciduous broadleaf shrubs (n = 32) in June and September. Results of paired sample t-tests of leaf SIRM between June and September are indicated by "***" p-value < 0.001. **(b)** Box plots for leaf SIRM of investigated plant types (n = 5) in September. For equal exposure time, the leaf SIRM of investigated deciduous plant species (n = 77) was adjusted by subtracting the June leaf SIRM from September leaf SIRM. The leaf SIRM of evergreen needle/scale-like, broadleaves and climber species was set to September leaf SIRM.

3.2 *Leaf traits LA, SLA, LDI, roundness, DCA and their relationship with leaf SIRM*

The LA ranged between 0.2 – 113.2 cm^2 in June, of which the smallest LA was observed for *J. communis* and largest for *Acer pseudoplatanus.* In September, the LA ranged between 0.1 – 182 cm^2 with the smallest LA for *Abies fraseri* and the largest for *Catalpa bignonioides*. The SLA ranged between 2.4 – 28.2 $m^2\ kg^{-1}$ in June and 3.8 – 23.6 $m^2\ kg^{-1}$ in September. The lowest SLA was observed for *C. deodara* and the highest for *Robinia pseudoacacia* in both June and September. The LDI ranged between 6.8 - 40.3 in June and 6.8 – 42.5 in September. In both June and September, the lowest LDI value was observed for *Lonicera tartarica* and the highest for *C. lawsoniana*. Higher LDI values were mostly associated with evergreen needle/scale-like species. The leaf roundness ranged from 0.03 – 0.9 in June with the smallest and largest value observed for *Cedrus deodara* and *Crataegus monogyna* respectively. In September, the leaf roundness ranged from 0.05 – 0.9 with the smallest and largest leaf roundness value observed for *Pinus nigra* and *C. monogyna* respectively. In June, the DCA (AB) ranged from 56 º - 147 º with the smallest and the largest DCA (AB) observed on the leaves of *Sambucus nigra* and *Elaeagnus angustifolia* respectively. In June, the DCA (AD) ranged from 56 ° - 136 ° with the smallest and the largest DCA (AD) observed on the leaves of *Corylus colurna* and *L. tartarica* respectively. In September, DCA (AB) ranged from 54 º - 130 º with the smallest and the largest DCA (AB) observed on the leaves of *S. nigra* and *Sorbus aria* respectively. In September, the DCA (AD) ranged from 51 º – 125 º with the smallest and the largest DCA (AD) observed on the leaves of *C. colurna* and *Rosa glauca* respectively (Table 2).

The PCA identified groups of plant species with similar anatomical and morphological characteristics, with the first two components of the PCA explaining 28.9 % and 19.6 % respectively of the variances. In the biplot (Fig. 4) plant species were segregated by the LDI and SLA in two distinct groups. One group consisting of deciduous and evergreen needle/scale-like species. While the other group consisted of deciduous broadleaf species. Further differentiation within the two clusters related to the DCA and the negatively correlated LA.

The MLR for June (Table 3), indicates the contribution of DCA [AB, AD], TD and SD in explaining the variation in leaf SIRM. In June, the leaf SIRM showed a significant negative relationship with the DCA [AB, AD] and the SD. While a significant positive relationship between the TD and leaf SIRM was indicated. In September, the MLR indicated a significant negative effect of SLA, DCA [AD], and a significant positive effect of TD.

As SLA is functional plant type-specific according to the PCA (Fig. 4), we aggregated the initial five functional plant types into a more condensed three functional plant types because the climber and evergreen broadleaf functional plant types consisted of a small number of plant species. Therefore, the three functional plant types were namely ‘evergreen needle/scale-like’, ‘deciduous broadleaf’ comprising of (deciduous broadleaf trees, shrubs, and deciduous needle-like), and ‘evergreen broadleaf’ consisting of climber and evergreen broadleaf species. We tested the relationship between leaf SIRM and SLA for the above-mentioned three functional plant types. A negative relationship between SLA and leaf SIRM was observed for the three functional plant types in September (Fig. 5).

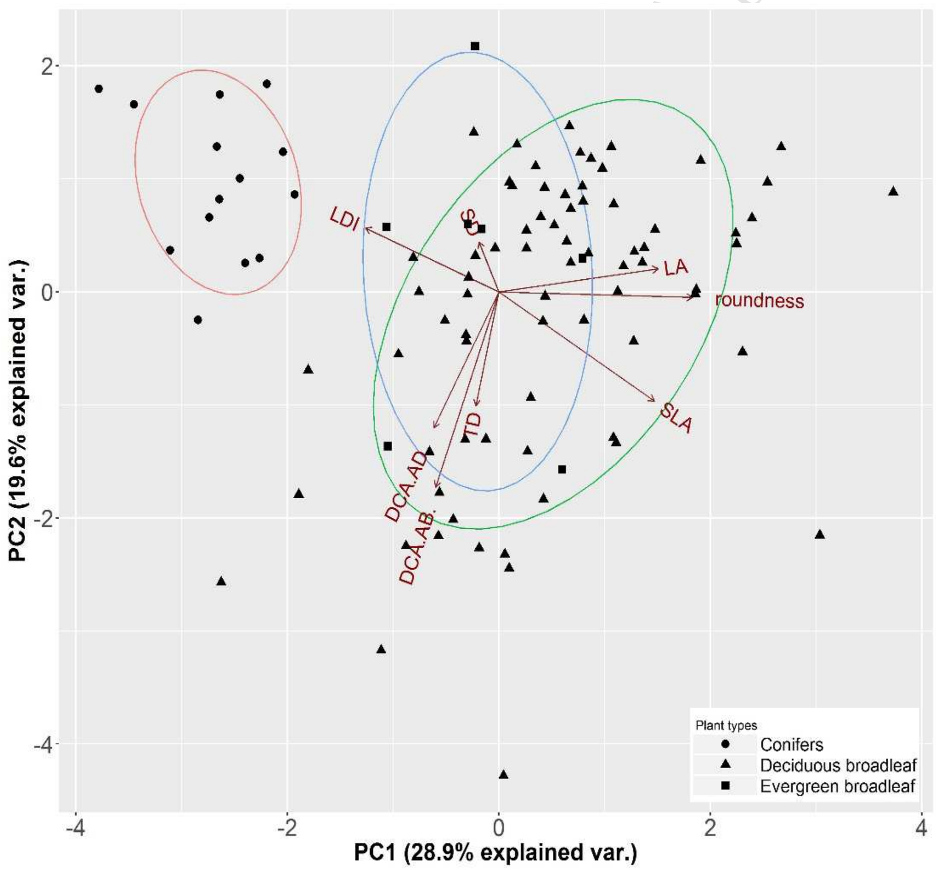

Fig. 4. Bi-plot of the principal component analysis on the anatomical and morphological variables measured at leaf level of the considered plant species (n = 96): leaf dissection index (LDI), leaf roundness

(roundness), single leaf area (LA), specific leaf area (SLA), drop contact angle at abaxial (DCA AB), and adaxial (DCA AD), trichome density (TD), stomatal density (SD). Principal Component 1 (PC1) explains 28.9 %, and PC2 explains 19.6 % of the variance.

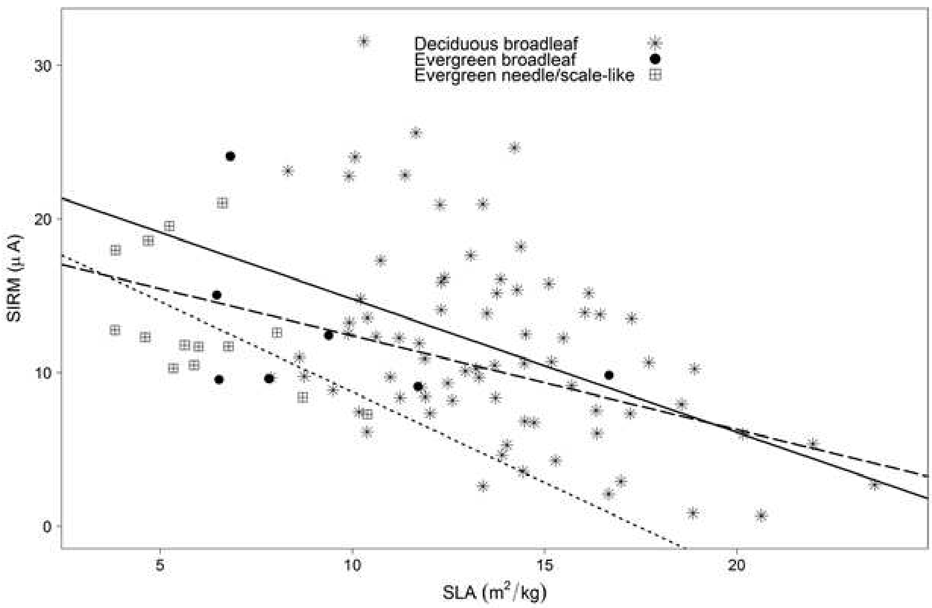

Fig. 5. SLA (m^2 /kg) in relation to leaf SIRM (µA) at species level for aggregated plant types (n = 3) evergreen needle/scale-like, deciduous trees and shrubs consisting of broadleaves and needle-like (n = 77, R^2 = 0.20, p < 0.001). Evergreen broadleaf consisting of evergreen shrub, tree and climber species (n = 7, R^2 = 0.17, p = 0.344). Evergreen needle / scale-like (n = 12, R^2 = 0.27, p = 0.051) in September 2016. Lines shown are regression lines – solid for deciduous broadleaf, dashed for evergreen broadleaf, dotted for evergreen needle/scale-like. SIRM values of investigated deciduous plant species are adjusted by subtracting the June leaf SIRM from the September leaf SIRM. The leaf SIRM of evergreen (needle/scale-like, broadleaves and climber species), was set to September leaf SIRM (see Table 2).

Table 3

Results of multiple linear regression (MLR) on leaf SIRM in June (for deciduous needle-like, broadleaf tree and shrub species), in September (for all investigated plant species) indicating the effect of leaf traits: specific leaf area (SLA), drop contact angle (DCA) [abaxial (AB) adaxial (AD)], leaf dissection index (LDI), stomatal density (SD) trichome density (TD), and leaf roundness, showing the estimate, standard error (SE), and the p-values. The leaf SIRM in June and September was transformed ln(SIRM). Significant effects (p-value ≤ 0.05) are shown in bold.

SIRM	Variable	Estimate	SE	p-value
June	Intercept	3.062×10^{0}	3.272×10^{-1}	**< 0.001**
(n = 77)	SLA	-1.660×10^{-2}	1.377×10^{-2}	0.232
	leaf roundness	-2.957×10^{-1}	2.212×10^{-1}	0.185
	DCA (AB)	-4.071×10^{-3}	1.994×10^{-3}	**0.045**
	DCA (AD)	-9.089×10^{-3}	3.777×10^{-3}	**0.018**
	SD	-6.421×10^{-4}	2.440×10^{-4}	**0.011**
	TD	8.054×10^{-5}	3.812×10^{-5}	**0.032**
September	Intercept	23.926×10^{0}	3.380×10^{0}	**<0.001**
(n = 96)	SLA	$- 5.001 \times 10^{1}$	1.345×10^{-1}	**<0.001**
	DCA (AD)	-8.711×10^{-2}	4.367×10^{-2}	**0.049**
	TD	1.138×10^{-3}	4.563×10^{-4}	**0.016**

3.3 *Stomatal density (SD) and trichome density (TD) and their relationship with leaf SIRM*

Leaves of a subset of species were analyzed for SD (n = 38) and TD (n = 51). Very few overlapping species (n = 7) with very sparse trichomes were analyzed for both SD and TD. Leaves of evergreen needle/scale-like, evergreen broadleaves and some deciduous broadleaf tree and shrub species with very sparse to no trichomes on their leaf surfaces were analyzed for SD. The SD between plant species ranged from 20 – 736 mm^{-2} (Table 2). The least amount of stomata were found on the leaves of *J. communis* and the greatest on *S. purpurea*. *Hibiscus syriacus* and *S. purpurea* were amphistomatous as stomata were present on both the abaxial and the adaxial leaf sides. For both of these amphistomatous species, the SD was higher on the AB leaf side. The remaining plant species were hypostomatous. The SD for evergreen broadleaf species ranged from 212 till 302 mm^{-2}, for evergreen needle/scale-like between 20 and 188 mm^{-2} and for deciduous broadleaf trees between 56 and 628 mm^{-2}. The MLR for June indicated, a significant negative effect of SD on leaf SIRM while the MLR for September indicated no significant effect of SD on leaf SIRM (Table 3).

The TD for species with countable trichomes ranged from 0.4 – 45.1 mm^{-2}. The lowest TD was observed for *Alnus glutinosa* and the highest for *E. angustifolia*. No trichomes were observed on the leaves of deciduous and evergreen needle/scale-like species (n = 14) and evergreen broadleaves (n = 4) except for *Q. ilex*. Six plant species, i.e., *B. davidii, Malus sylvestris, Q. ilex, Salix rosmarnifolia, S. aria,* and *Sorbus intermedia* had a dense network of hairs on their leaf surfaces, for which TD could not be determined. In September, a general trend of higher leaf SIRM values was observed for plant species with a dense network of trichomes compared to plant species with lower TD (Fig. 2, Table2). The MLR for June and September indicated a significant positive effect of TD on leaf SIRM (Table 3).

3.4 *Differences in leaf SIRM between clusters based on leaf traits*

Based on the leaf characteristics (LDI, SD, TD, LA, SLA, leaf roundness, and DCA [AB, AD]) measured in both June and September with the exception of TD and SD which were measured once during the growing season, five clusters could be delineated within the 96 investigated plant species (Fig. 6). The dendrogram obtained in June was fairly identical to the dendrogram obtained in September with the exception of *Taxus baccata* which was located in cluster 3 in June and cluster 2 in September. Cluster 1 consisted of plant species with a dense network of trichomes, plant species in cluster 2 generally had an SLA ≥ 7.0, cluster 3 consisted of deciduous and evergreen needle/scale-like, cluster 4 consisted of plant species with high leaf wettability, i.e., small DCA (< 90°) on both the AB and the AD leaf sides while plant species in cluster 5 had non-wettable leaves, i.e., a large DCA (> 90 °) on both the AB and the AD leaf sides. In June, the median leaf SIRM of cluster 3 being 23.4 µA was significantly higher (Table 4) than that of cluster 1 (7.3 µA), cluster 2 (4.5 µA), cluster 4 (5.6 µA) and cluster 5 (4.7 µA). In September, the median leaf SIRM of cluster 1 being 23.8 µA was significantly higher from clusters 2 (12.9 µA), 3 (12.3 µA) and 5 (14.7 µA), while the leaf SIRM of cluster 2 differed slightly from cluster 4 (16.2 µA) but did not differ from cluster 3 and 5.

Table 4
Results of the post-hoc test following ANOVA for testing differences in the leaf SIRM between five clusters of selected plant species (n = 96) based on leaf traits (see Fig. 6 for an explanation of cluster codes) for the leaf SIRM in June and September. Significant differences (p-value ≤ 0.05) are shown in bold.

Cluster comparison	June p- value	September p- value
Cluster 2 – Cluster 1	0.636	**0.005**
Cluster 3 – Cluster 1	**<0.0001**	**0.007**
Cluster 4 – Cluster 1	0.803	0.289
Cluster 5 – Cluster 1	0.559	**0.016**
Cluster 3 – Cluster 2	**<0.0001**	0.999
Cluster 4 – Cluster 2	0.986	**0.055**
Cluster 5 – Cluster 2	0.999	0.956
Cluster 4 – Cluster 3	**<0.0001**	0.118
Cluster 5 – Cluster 3	**<0.0001**	0.952
Cluster 5 – Cluster 4	0.956	0.242

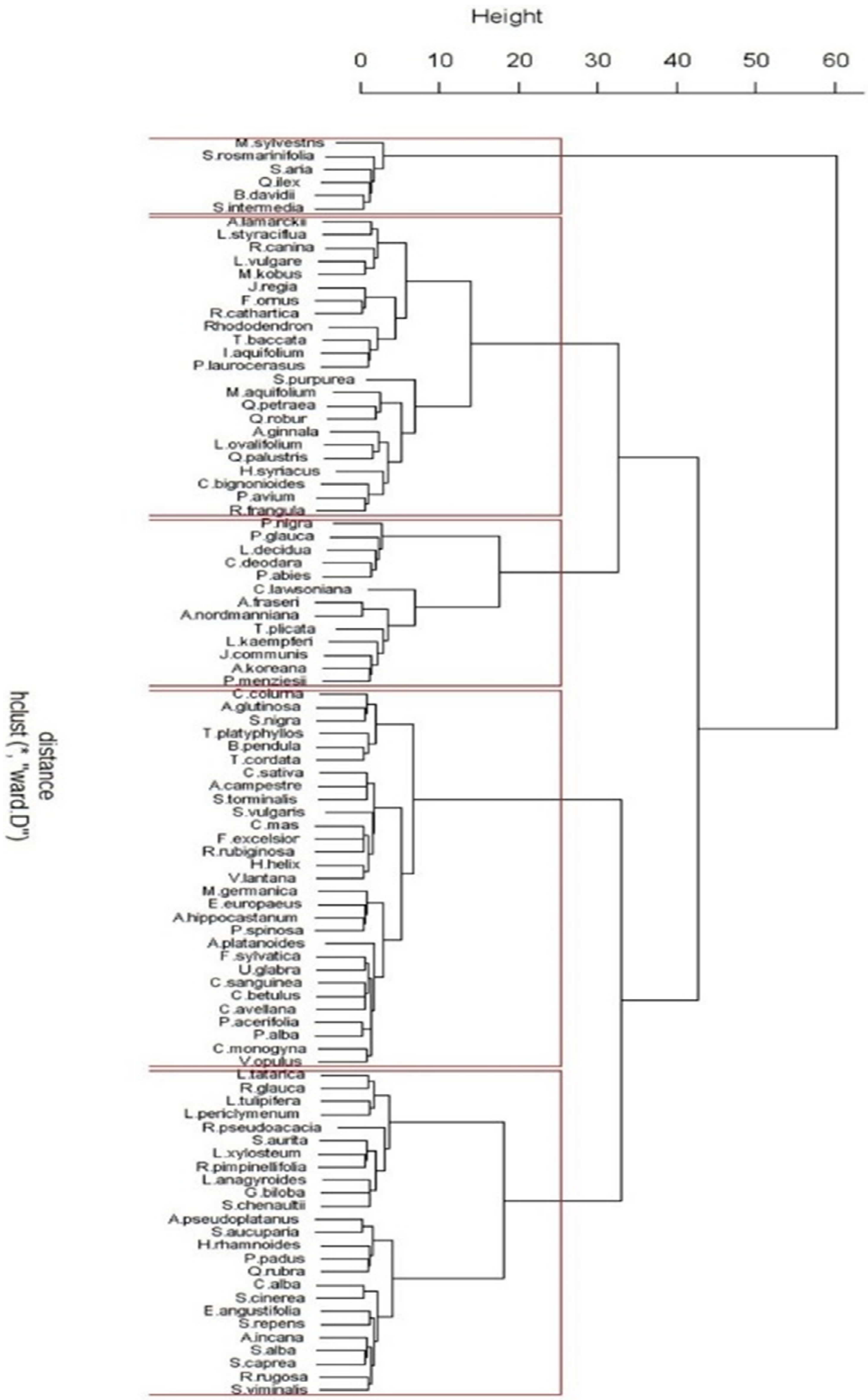

Fig. 6. Multivariate cluster analysis dendrogram in September using the Ward algorithm. Cluster 1 - 5 in order of appearance from top to bottom.

3.5 *Variable importance using randomForest on leaf SIRM classes*

The RF algorithm was applied on nine data subsets (Table 1; Fig. 7). The leaf SIRM was grouped into three classes, i.e., (low, medium, and high leaf SIRM) using quantile classification. The SLA was observed to be the VI across the nine RF subsets. Therefore, we tested the performance of RF models by eliminating SLA as an explanatory variable. It was observed that the OOB error rate increases for the subset with deciduous broadleaf species from ~ 39.4 to 52 % and evergreen species from ~ 22.6 to 49 %. With the incorporation of SLA, the OOB error rate ranged from 22.6 – 49.1 % across the nine RF subsets. The presence of leaf hairs, SLA, and leaf roundness was observed to be VI for the AS data subset consisting of all plant species (n = 96) with an OOB rate of 45.1% (Fig. 7a). The RF for the broadleaf datasets (BJ, BS, BD) (Fig. 7b) indicated an OOB error rate of 39.4 – 44.6% (Fig. 7d, e, f) with VI highest for SLA, DCA (AB), and DCA (AD). The dataset EJ and ES consisted of evergreen needles/scale-like, broadleaves, and climber species with the lowest OOB error rate of 22.6 – 39.2 % (Fig. 7b, c). For the evergreen species, the VI was observed for SLA and leaf type, i.e., needle/scale-like or broadleaves. For the AS-SD subset, the OOB error rate was 40.8% (Fig. 7g), and the VI was observed for SLA, DCA (AD), and LDI. Finally, the RF was applied on plant species exclusively accounted for trichome density (DEBS-TD and DEBD-TD), the OOB error rate was 41.4 – 49.1% (Fig. 7h, i) and SLA was the variable of importance.

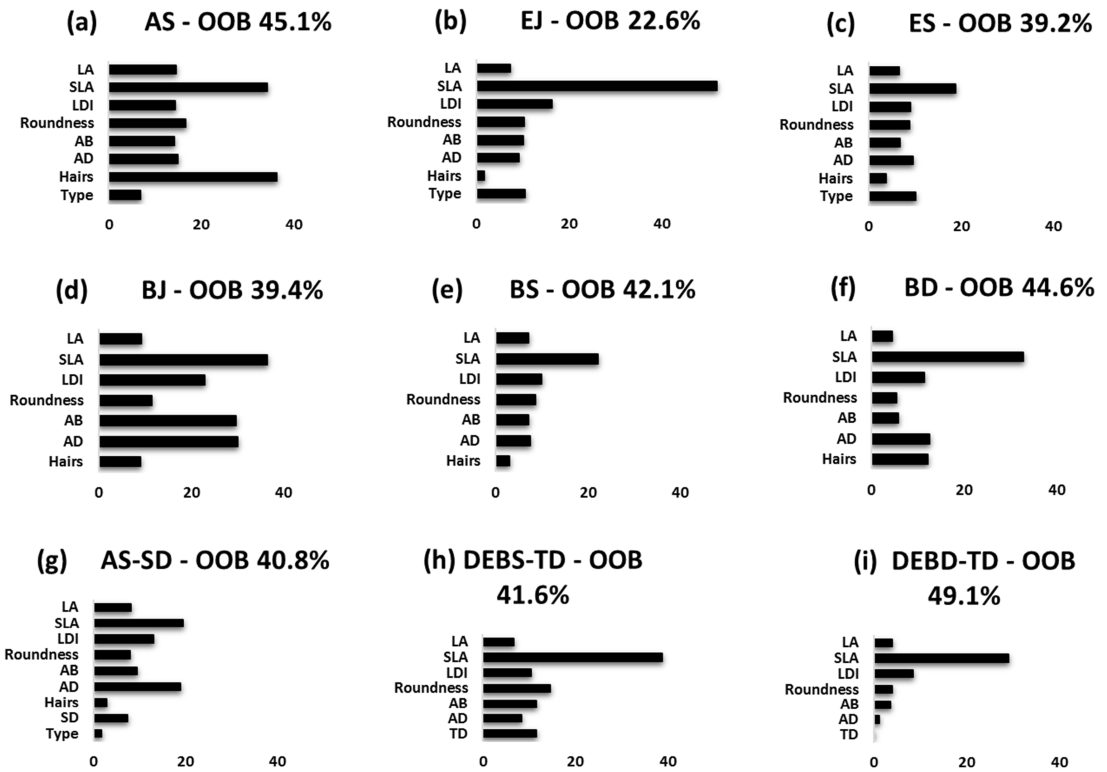

Fig. 7. Mean Decrease Accuracy (MDA) values shown from 0 – 40 (Low value = less important, High value = more important) for the explanatory variables i.e. leaf area (LA), specific leaf area (SLA), leaf dissection index (LDI), leaf roundness, Drop contact angles – abaxial (AB) and adaxial (AD), presence of trichomes (Hairs), stomatal density (SD), trichome density (TD), type of leaf (needle, scale-like and broadleaves). The Out-of-bag error rate (OOB) for nine subsets of data (see Table 1) with leaf SIRM grouped as (low, medium, high) using quantile classification. (AS = all plant species in September, BJ = Broadleaves in June, EJ = evergreens in June, BS = Broadleaves in September, ES = evergreens in September, BD = ∆SIRM for broadleaves, AS-SD = species with SD data in September, DEBS-TD = deciduous /evergreen broadleaves species in September with TD data, DEBD- TD = deciduous /evergreen broadleaves species for ∆SIRM with TD data.

a

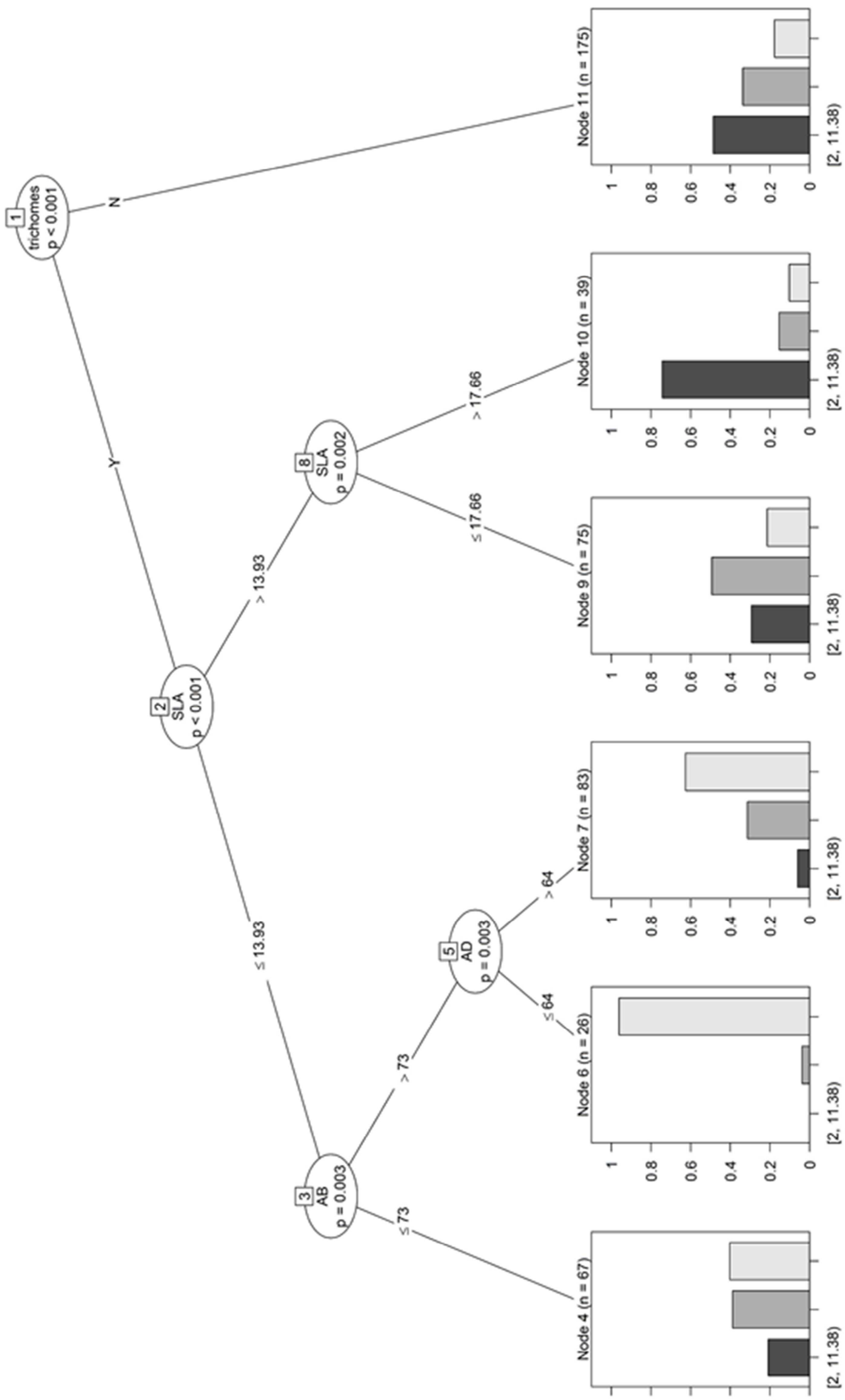
1
trichomes
p < 0.001
N
Y
2
SLA
p < 0.001
≤ 13.93
> 13.93
3
AB
p = 0.003
≤ 73
> 73
5
AD
p = 0.003
≤ 64
> 64
8
SLA
p = 0.002
≤ 17.66
> 17.66
Node 4 (n = 67)
Node 6 (n = 26)
Node 7 (n = 83)
Node 9 (n = 75)
Node 10 (n = 39)
Node 11 (n = 175)
[2, 11.38)
1
0.8
0.6
0.4
0.2
0

b

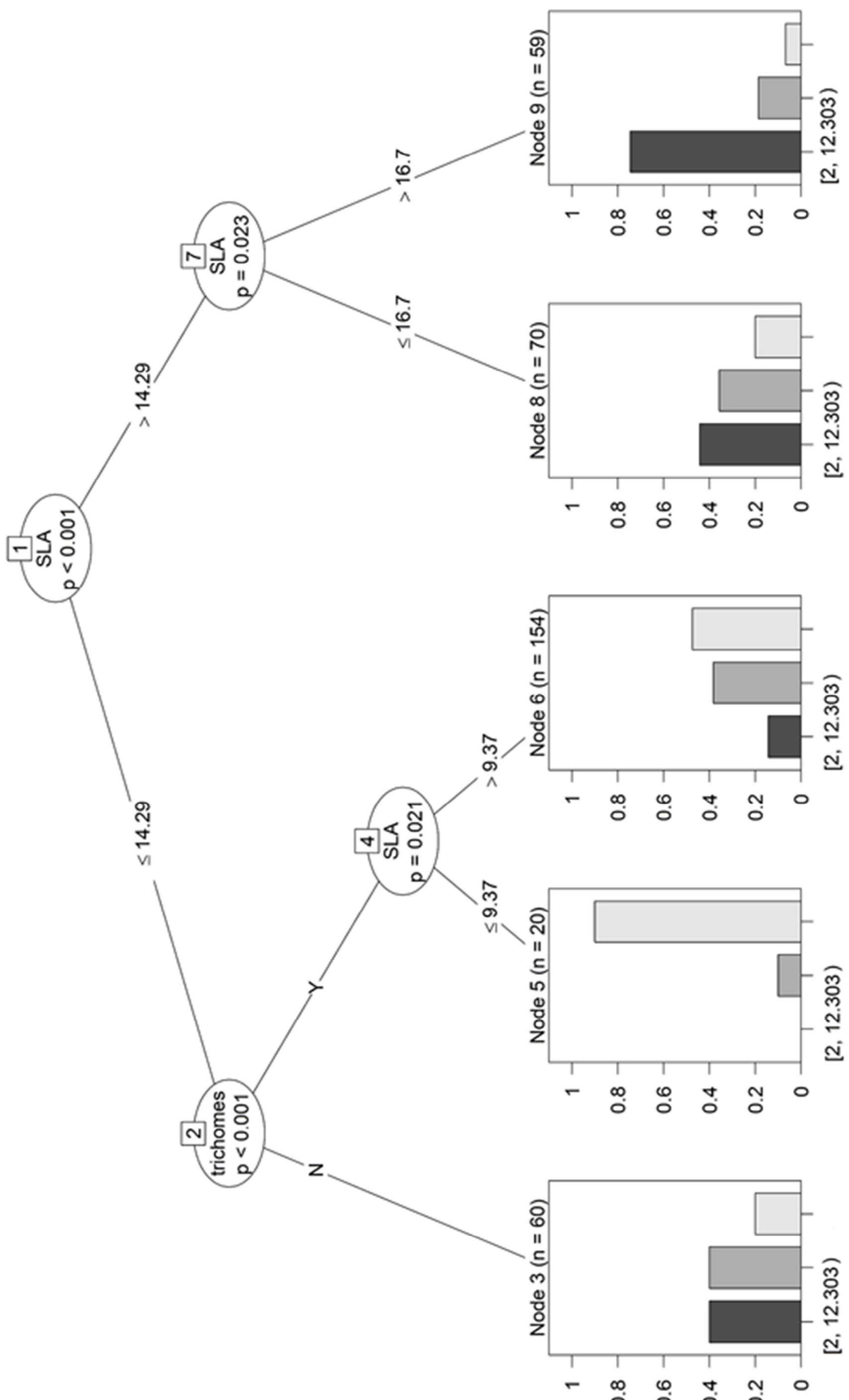
1
SLA
p < 0.001
≤ 14.29
> 14.29
2
trichomes
p < 0.001
N
Y
4
SLA
p = 0.021
≤ 9.37
> 9.37
7
SLA
p = 0.023
≤ 16.7
> 16.7
Node 3 (n = 60)
Node 5 (n = 20)
Node 6 (n = 154)
Node 8 (n = 70)
Node 9 (n = 59)
[2, 12.303)
0
0.2
0.4
0.6
0.8
1

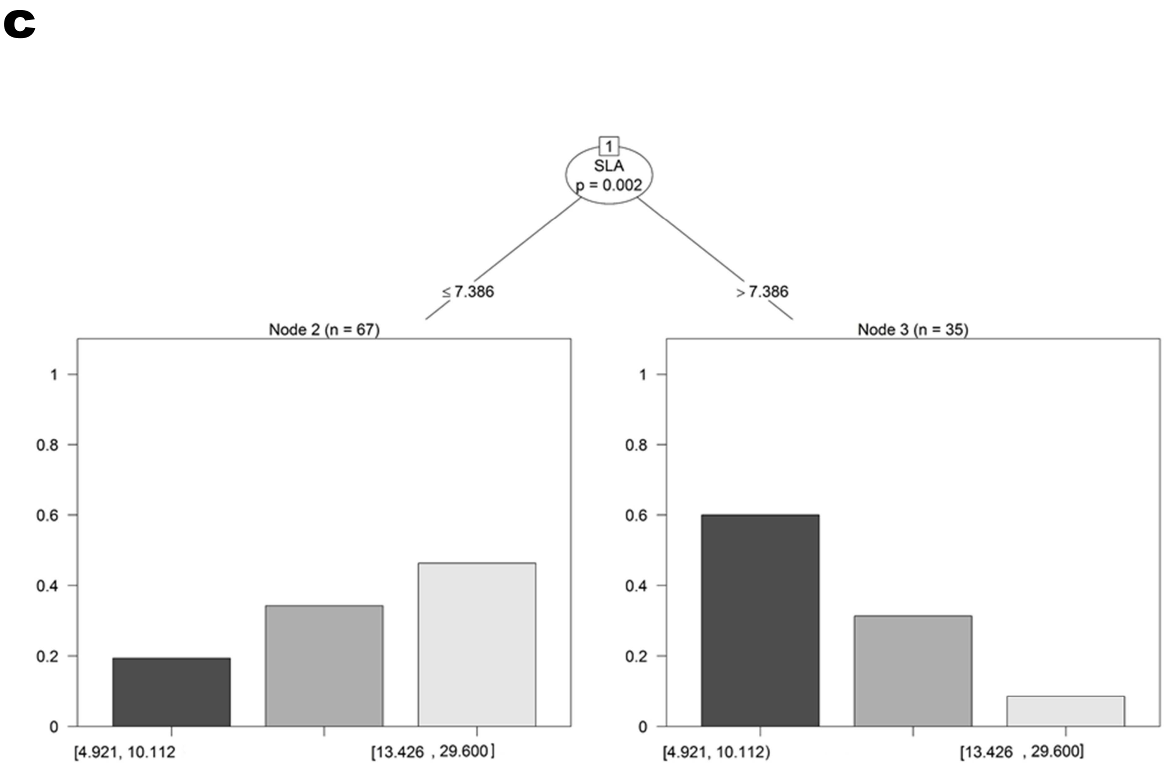

Fig. 8. Decision trees to classify plant species according to leaf SIRM grouped into three classes using quantile classification low (dark gray), medium (gray) and high (light gray) in September for (a) all investigated plant species (b) deciduous broadleaf tree and shrub species (c) evergreen needle/scale-like, broadleaf, and climber species. The nodes in the decision tree represent plant species classification within the three leaf SIRM classes, and the branches of the nodes represent the decision rules or conditions.

4. Discussion

The set-up of the experiment as a common-garden setting enabled us to compare the net particle accumulation abilities for a wide array of plant species with contrasting leaf surface morphology placed in a spatially uniform environment. Doing so, we were able to avoid bias due to external sources, i.e., vehicular traffic, railways, industries causing an influence on atmospheric particle concentrations. Moreover, the confounding factors of shade, light, wind speed, air temperature, and humidity were avoided. Hence, an impartial comparison in net particle accumulation between plant species was facilitated.

4.1 *Inter-species differences in net particle accumulation*

All plant species investigated in this study showed a net accumulation of atmospheric particles on their leaf surfaces as assessed by leaf SIRM. The leaf SIRM ranged between 0.7 – 31.6 µA with the lowest leaf SIRM observed on the leaves of *P. alba* and the highest on the leaves of *B. davidii* in September. Low net particle accumulation on the leaves of poplar in both coarse and fine particulate size fraction was also observed by Beckett et al. (2000). In the same study, *S. aria* was identified as the most effective accumulator of coarse particulates. Although we did not differentiate between particle size fraction of PM but observed a high leaf SIRM for *S. aria* in September. A leaf SIRM of 6.8 µA was observed in our study for *Betula pendula* in September which was within the range observed by Matzka and Maher (1999). In our research, a leaf SIRM of 2.1 µA was observed for *Platanus x acerifolia* in September while Hofman et al. (2013) observed leaf SIRM values between 3.5 – 64.1 µA. These discrepancies can be attributed to the examined study area with different air pollution concentrations. The present study was conducted in a common-garden setting away from specific pollution sources whereas, Hofman et al. (2013) conducted the leaf sampling in a street canyon in the city of Ghent, Belgium. Our study corroborates the findings of Kardel et al. (2011) for *Tilia cordata*, *T. platyphyllos,* and *Carpinus betulus*. The leaf SIRM values obtained in our study for the above-mentioned plant species were in the same order of magnitude(Table 2, Fig. 2) as observed by Kardel et al. (2011) in urban habitats with low air pollution. Low net particle accumulation was observed on the leaves of *R. pseudoacacia* in both June and September as was reported by Sæbø et al. (2012). Plant species such as *Quercus rubra*, *C. bignonioides* with low net particle accumulation on their leaf surfaces (Table 2, Fig. 2) were grouped into the least effective ("Low") group of plant species. Similar results for *Q. rubra* and *C. bignonioides* were reported by (Popek et al. 2013). Results from our study also corroborate the findings of Mitchell et al. (2010) for *T. platyphyllos* and *Fagus sylvatica* showing a high net particle accumulation whereas, *Castanea sativa*, *Salix alba,* and *S. nigra* were observed to have a medium net particle accumulation (Fig. 2).

The leaf SIRM of evergreen: needle/scale-like, broadleaves and climber species ranged between 9.1 – 24.1 µA in September. The lowest leaf SIRM was observed on the leaves of *H. helix* while the highest leaf SIRM was observed on the leaves of *Q. ilex* an evergreen broadleaf. Plant species such as *Q. ilex, Pseudotsuga menziesii*, *Thuja plicata*, *J. communis, Picea pungens glauca* and *Rhododendron* were observed to be in the most effective ("High") group of net particle accumulators (Fig. 2). Moreno et al. (2003) performed a magnetic analysis on the leaves of a deciduous (*Platanus* sp) and an evergreen (*Q. ilex*) species. The authors revealed that leaves of an evergreen plant species show a higher magnetic intensity possibly due to the extended lifespan of their leaves compared to the leaves of deciduous plant species. Although, the differences in net particle accumulation between functional plant types (evergreens versus deciduous plant species) have been reported in the past by, e.g., Freer-Smith et al. (2005); Cavanagh et al. (2009); Sæbø et al. (2012); Przybysz et al. (2014) but the age of leaves may have been seemingly overlooked. Our study provides a comparison of net particle accumulation between plant species with leaves of similar age. Because leaves of some deciduous plant species can also be effective net particle accumulators as identified in our study (Fig. 2).

4.2 *Differences between functional plant types and families in net particle accumulation*

Differences in leaf SIRM of deciduous broadleaf tree and shrub species from June to September were examined (Fig. 3a). The paired sample t-test for broadleaf tree and shrub species indicated a significant ($p < 0.001$) increase in leaf SIRM from June till September. An increase in leaf SIRM on the leaves of broadleaf tree and shrub species was likely due to the presence of leaf trichomes. Dzierzanowski et al. (2013) examined particle mass on leaves of trees, shrubs, and climber species and observed that shrubs were more effective in particle accumulation whereas, the climber species accumulated the smallest amount of particle mass on their surfaces and in their wax layer. In the present study, the mass of particles was not estimated, but the climber species with a median leaf SIRM of 9.5 µA were observed to be the least net particle accumulating plant species. Thus, corroborating the findings of Dzierzanowski et al. (2013). No significant differences between the leaf SIRM of deciduous broadleaf tree and shrub species were observed in June and September. As expected, the leaf structure of both functional plant types does not differ systematically. Additionally, the net particle accumulation mainly depends on leaf characteristics. Sæbø et al. (2012) examined plants which were bought from nurseries and grown in pots for differences in PM accumulation also found no significant differences between the leaves of deciduous broadleaf tree and shrub species. When comparing leaf SIRM of investigated functional plant types ($n = 5$) with equal exposure time, no significant differences were observed (Fig. 3b).

The leaf SIRM differed at plant family level. Species belonging to the Adoxaceae and Betulaceae showed a high leaf SIRM, which might be explained by the wettable character of their leaves. Species belonging to the Fabaceae and Caprifoliaceae had a low leaf SIRM due to the non-wettable character of their leaf surfaces. Besides, intra-family differences in leaf SIRM were also observed. For example, in the family Rosaceae, *Rosa rugosa* and *S. aria* were observed to have a high leaf SIRM while *Prunus* *laurocerasus* relatively had a low leaf SIRM. This intra-family variation can be attributed to the presence of trichomes on the leaves of *R. rugosa* and *S. aria* whereas, the leaves of *P. laurocerasus* were very smooth with no trichomes. Similar observations were noted for the family Fagaceae. The plant families mentioned above were some examples because intra-family variations were frequently observed due to differences in leaf surface characteristics of the respective family members.

4.3 *Seasonal variation in net particle accumulation*

The leaf SIRM of deciduous needle-like, broadleaf tree and shrub species (n = 77) ranged from 1.3 – 15.7 µA in June and 0.7 – 31.6 µA in September. Thus, indicating a steady increase in leaf SIRM on average of about 218 % with time (Fig. 3a). It should be noted that since leaf surfaces remain in constant contact with the atmosphere and are prone to varying meteorological conditions. Therefore the leaf deposited particles would be subjected to repeated episodes of re-suspension due to wind or wash-off due to rain. Therefore, the leaf SIRM values obtained in this study should not be considered final or depict a linear accumulation trend with time. However, particles which immobilize within the wax layer (Hofman et al. 2014), affixed on leaf trichomes/hypahe of fungi or encapsulated within the stomatal cavities, the re-suspension of those particles by rain or wind would be negligible (Hofman et al. 2014). We did not estimate the immobilized or encapsulated portion of particles which warrants future research. Our results were in-line with the study of Kardel et al. (2011) where the examined deciduous plant species showed an increase in leaf SIRM with time during the growing season (June till September). Hofman et al. (2014) examined the leaf SIRM of *P. acerifolia* for an entire growing season and observed short-term fluctuations but with a steady increase in leaf SIRM was observed until the onset of senescence. Hofman et al. (2014) attributed these fluctuations to leaf developmental stages. The authors also elaborated the importance of leaf exposure time for the steady increase in leaf SIRM as was reported by McIntosh et al. (2007). Although, we did not assess the temporal/seasonal dynamics of leaf SIRM but results of equal exposure time (section 3.1) in September for the investigated plant species (n = 96) indicated a steady increase in leaf SIRM (Fig. 2).

4.4 *Leaf characteristics and leaf SIRM*

We analyzed the effect of leaf surface characteristics on leaf SIRM. It was revealed that species-specific leaf traits primarily governed the differences in leaf SIRM between plant species. These findings were substantiated by MLR (Table 3), cluster analysis as well as the obtained decision trees (section 3.4, 3.5 respectively). The post-hoc Tukey-HSD test (Table 4) indicated that leaf SIRM of cluster 1 (Fig. 6) consisting of plant species with dense trichomes was significantly higher than leaf SIRM of cluster 2, 3 and 5. The leaves of deciduous broadleaf tree and shrub species with trichomes on their surfaces consistently showed high leaf SIRM in both June and September while low leaf SIRM values were mainly observed for the plant species having hydrophobic leaf surfaces (Fig 2, Table 3). Hence, validating our hypothesis (b and c) that leaf SIRM increases with an increase in trichome density and reduces with an increase in hydrophobicity. Leaves of six plant species with a dense network of trichomes (section 3.3) for which we were unable to measure the TD also had a high leaf SIRM with *B. davidii* having the highest leaf SIRM in September. The significance of trichomes in particle accumulation has also been reported by (e.g., Beckett et al. 2000; Mitchell et al. 2010; Kardel et al. 2011; Saebo et al. 2012). Song et al. (2015) identified that trichomes on the leaf surfaces were an optimum zone for particles to be deposited as they can be rough and adherent. De Nicola et al. (2008) suggests that trichomes increase the surface area in which the atmospheric particles may be deposited. Bakker et al. (1999) explained the relatively adequate particle deposition on hairy leaf surfaces by a decrease in leaf boundary layer resistance resulting in effective particle capture. While the studies mentioned above have elaborated the importance and contribution of leaf trichomes at a categorical level (dense, sparse, no-hairs). In this study, TD was quantitatively assessed for a large number of plant species (n = 51). For the first time, this has enabled the definition of a threshold value for TD and its effect on net particle accumulation. We observed that a TD ≤ 0.58 mm^{-2} would likely result in low net particle accumulation (Table 2). However, it was also observed that leaves of few plant species having both a high TD and low leaf wettability resulted in a low net particle accumulation (Table 2).

The effect of leaf wettability on leaf SIRM was significantly negative (Table 3). Plant species such as *L. tulipifera, Lonicera periclymenum, R. pseudoacacia, R. glauca,* and *Symphoricarpos x chenaultii* maintained non-wettable (DCA > 90 °) leaf surfaces on both sides of the leaf (Table 2) and were aggregated in cluster 5 (Fig. 6). Hence low leaf SIRM values were observed for the above-mentioned plant species in both June and September (Table 2). Neinhuis and Barthlott (1998) measured particle densities along with leaf wettability and revealed that *Ginkgo biloba* with non-wettable leaf surfaces accumulated fewer particles whereas, *Quercus robur* and *F. sylvatica* with wettable leaf surfaces, had a high particle density. Our study corroborates these findings. We also observed that leaf wettability increased from June to September for the majority of plant species, possibly increasing the efficiency of net particle accumulation throughout the growing season. Although, leaf wettability was observed to be a good indicator for differences in net particle accumulation in early summer, but late summer sampling can provide pronounced differences in net particle accumulation between plant species. Increase in leaf wettability was observed on both sides of the leaf, but predominantly on the adaxial leaf surface (Table 2). This can be explained by the orientation of the adaxial leaf surfaces in space. They usually will be more directly exposed to weather conditions such as rain, solar radiation, and atmospheric particulates compared to the abaxial leaf sides. Hence, it might be expected that the wax-layer at the adaxial leaf sides may be more abrased or eroded resulting in an increase in leaf wettability (Kardel et al. 2012) compared to abaxial leaf side.

The MLR did not indicate a significant effect of LDI in both June and September. We, therefore, reject our hypothesis (a) that net particle accumulation increases with leaf shape complexity. Results from our study were in agreement with Leonard et al. (2016) who observed the highest PM mass on lanceolate shaped (the broadest part below the middle of the leaf) than on needle-like or linear leaves. Weerakkody et al. (2018) also observed relatively poor PM accumulation on elliptical and linear leaves. As a possible explanation, the authors suggest that leaves with large perimeters tend to bend more readily with wind flow (Weerakkody et al. 2018). Earlier studies of (Beckett et al. 2000; Freer-Smith et al. 2004, 2005; Räsänen et al. 2013; Mori et al. 2015) indicate that evergreen needle/scale-like species due to their aerodynamic leaf shape, and supposedly reduced boundary layer were effective accumulators of PM. However, results from our study suggest that other underlying factors such as trichome density and leaf wettability were of equal importance in net particle accumulation on leaf surfaces.

We did not observe any significant relationship between single leaf area and leaf SIRM ($p > 0.05$) in both June and September. However, a significant negative relationship ($p < 0.001$) between leaf SIRM and SLA (Table 3, Fig. 5) was observed for the MLR in September. The decision tree obtained using ® randomForest for deciduous broadleaf plant species (Fig. 8b) also indicates that leaves with low SLA were classified into a class with the high leaf SIRM. Sæbø et al. (2012) observed a significant negative relationship with SLA and leaf accumulated total PM, $PM_{10,}$ and $PM_{2.5}$ mass but a positive for $PM_{0.2}$ size fraction. Although we observed a significant negative relationship between SLA and net particle accumulation but our methodology does not distinguish between particle size fractions. Previous studies have shown SLA to vary within a plant species due to several environmental factors, such as water and nutrient availability (Wright et al. 2004; Poorter et al. 2009), shade (Balasooriya et al. 2009; Wuytack et al. 2011), temperature (Poorter et al. 2009), urban environments (Kardel et al. 2011). Therefore, caution should be exercised when predicting the net particle accumulation ability of a plant species collected from differing environmental conditions. The relationship between net particle accumulation and SLA can best be explained in conjunction with LDI. Leaves of evergreen needle/scale-like species predominantly have complex leaf structure resulting in high LAI, LAD, low SLA and supposedly reduced leaf boundary layer resistance which enhances net particle accumulation (Beckett et al. 2000; Freer-Smith et al. 2004, 2005; Sæbø et al. 2012).

For June, the MLR indicated a significant negative effect of SD on leaf SIRM, but no effect of SD was indicated for September. We were able to include imprints of 38 out of 96 plant species as the presence of dense trichomes hampered in obtaining good quality imprints. SD in our study for evergreen broadleaf species ranged from 212 till 302 mm^{-2}, for evergreen needle/scale-like between 20 and 188 mm^{-2} and deciduous broadleaf trees between 56 and 628 mm^{-2}. These ranges were in line with those specified by (Larcher 2003) for evergreen broadleaf (200 – 600 mm^{-2}), evergreen needle/scale-like (40 – 120 mm^{-2}), deciduous broadleaf trees (100 – 300 with a maximum limit of 600 mm^{-2}). Although particles can block stomata and can accumulate in stomatal cavities (Lehndorff et al. 2006; Song et al. 2015), we did not find any conclusive relationship between stomatal density and net leaf particle accumulation.

Conclusion

Plant species with a combination of leaf traits such as high trichome density and leaf wettability can enhance particle deposition and thus help in mitigation of atmospheric PM. We conclude that these positive leaf traits of plant species can be additive when utilizing them as PM filters. The differences in net particle accumulation between plant species were determined and expressed as leaf SIRM. The limitation of leaf SIRM was that the overall mass of PM accumulated on leaf surfaces could not be estimated. We considered the fact that leaf SIRM estimates only the ferro-magnetic and magnetizable component of PM which can be of exceptional importance due to its adverse health effects. The leaf SIRM was adequately capable of assessing the differences in net particle accumulation between plant species. The common-garden setting provided us with an impartial comparison by exposing all selected plant species to uniform climatic and atmospheric conditions. We were able to identify leaves of plant species those were the least and the most effective in net particle accumulation. Hence, when planning urban green infrastructures with an aim to reduce atmospheric PM informed choices can be made. The differences in net particle accumulation between plant species could largely be explained by their underlying leaf traits. The low leaf SIRM values were mainly observed for the plant species with non-wettable leaf surfaces. Leaves of deciduous broadleaf tree and shrub species with trichomes on their surfaces consistently showed a higher leaf SIRM in both June and September compared to leaves of those plant species which had no trichomes. Leaf trichomes typically play an enhanced role in particle capture as observed in the present study and that of Beckett et al. (2000); Mitchell et al. (2010); Dzierzanowski et al. (2011); Kardel et al. (2011); Sæbø et al. (2012); Popek et al. (2013). However, it was also observed that the leaves of some plant species with high trichome density and low wettability showed low leaf SIRM. This outcome from our study warrants further research to differentiate between waxy/non-waxy trichomes which may be a source of variation in leaf SIRM.

The decision trees obtained in our study indicated that the absence of trichomes was the first indicator of low effectiveness of a plant species in net particle accumulation. Next, the distinction between low and high net particle accumulators was made based on SLA. Since the presence of trichomes and SLA remain easy-to-measure leaf traits which involve very few resources and expertise. Thus, the assessment of the net particle accumulation abilities can be reasonable and efficiently done following the obtained decision trees. However, earlier studies have indicated that SLA can be influenced by environmental factors (Wright et al. 2004; Poorter et al. 2009; Balasooriya et al. 2009; Wuytack et al. 2011; Kardel et al. 2011). Therefore, caution should be exercised when predicting the net particle accumulation abilities of a plant species collected from differing environmental conditions. The generated decision trees are of high value because of their applicability in assessing the abilities of un-examined plant species found either locally or regionally.

At leaf level, the micro-morphology of leaves such as trichomes, wettability, roughness, waxes, can enhance particle capture (Mitchell et al. 2010; Kardel et al. 2011; Dzierzanowski et al. 2011; Sæbø et al. 2012; Grote et al. 2016; Neinhuis and Barthlott 1997). At canopy level, leaf area index (LAI) defined as leaf area per unit ground surface and PM deposition on barks and stems, should be incorporated as they indicate the potential plant area for deposition. Also, the size and structure, e.g., leaf area density (LAD) defined as total one-sided leaf area per unit of layer volume, of tree crowns increase turbulent air movements which influence the particle deposition on leaves (Fowler et al. 1989) is of importance. To the best of our knowledge, this is the first study to compare such a wide array of plant species (n = 96) at leaf level to discern inter-species differences in net particle accumulation. Outcomes from our research study can empower city planners in optimizing urban green designs by selecting the most effective plant species to mitigate atmospheric PM pollution.

Acknowledgments

The research was funded by the Ontario Student Assistance Program (OSAP # 15103399). The authors would like to thank Dr. Simo Spassov for facilitating the magnetic measurements in their laboratory at the Royal Meteorological Institute of Belgium, Dourbes, Belgium. Prof. em. Roland Caubergs for helping with the leaf clearing protocol and Prof. dr. Stefan Van Dongen for his valuable comments on data treatment. The authors acknowledge the help of master students Ellen Soetens and Catherine Brück involved in this project and the ENdEMIC group involved in the upkeep of the experimental site. The authors would like to thank the anonymous reviewers for their critical comments and constructive suggestions in improving the article.

References

Air quality in Europe. 2015. European Environment Agency ISBN 978-92-9213-702-1 Page 9.

Bakker, M.I., Vorenhout, M., Sijm, D.T.H.M., Kollöffel, C., 1999. Dry deposition of atmospheric polycyclic aromatic hydrocarbons in three Plantago species. Environmental Toxicology and Chemistry 18: 2289 – 94.

Balasooriya, B.L.W.K., Samson, R., Mbikwa, F., Vitharana, W.A.U., Boeckx, P., VanMeirvenne, M., 2009. Biomonitoring of urban habitat quality by anatomical and chemical leaf characteristics. Environmental and Experimental Botany 65: 386 - 394.

Barima, Y.S.S., Angaman, D.M., N'Gouran, K.P., Koffi, N.A ., Kardel, F., De Cannière, C ., Samson, R. 2014. Assessing atmospheric particulate matter distribution based on saturation isothermal remanent magnetization of herbaceous and tree leaves in a tropical urban environment. Science of Total Environment 470–471: 975 – 982

Beckett, K.P., Freer-Smith, P.H., Taylor, G., 2000. Effective tree species for local air quality management. Journal of Arboriculture. 26: 12 - 19.

Beckett, K.P., Freer-Smith, P.H., Taylor, G., 1998. Urban woodlands: their role in reducing the effects of particulate pollution. Environmental Pollution 99: 347 - 360.

Bosko, ML., Varrica, D., Dongorra´, G., 2005. Case study: inorganic pollutants associated with particulate matter from an area near a petrochemical plant. Environmental Research 99: 18 - 30.

Breiman, L., 2001. Random forest. Machine Learning 45: 15 – 32.

Burkhardt, J., 2010. Hygroscopic particles on leaves: nutrients or desiccants? Ecological Monographs 80: 369 - 399.

Cavanagh, J.A.E., Zawar-Reza, P., Wilson, J.G., 2009. Spatial attenuation of ambient particulate matter air pollution within an urbanised native forest patch. Urban Forestry and Urban Greening 8: 21 - 30.

Chen, L., Liu, C., Zhang, L., Zou, R., Zhang, Z., 2017. Variation in tree species ability to capture and retain airborne fine particulate matter (PM2.5). Nature – Scientific Reports 1 – 11.

Cutler, D.R., Edwards, T.C., Beard, K.H., Cutler, A., Hess, K.T., Gibson, J., Lawler, J.J., 2007. Random forests for classification in ecology. Ecology 88: 2783 – 2792.

De Nicola, F., Maisto, G., Prati, M.V., Alfani, A., 2008. Leaf accumulation of trace elements and polycyclic hydrocarbons (PAHs) in Quercus ilex L. Environmental Pollution 153: 376 – 83.

Dzierzanowski, K., Popek, R., Gawronska, H., Saebo, A., Gawronski, S.W., 2011. Accumulation of particulate matter by several plant species in regard to PM fractions and deposition on leaf surface and in waxes. Int. International Journal of Phytoremediation 13: 1037- 1046.

Fowler, D., Cape, J.N., Unsworth, M.H., 1989. Deposition of atmospheric pollutants on forests. Philosophical Transactions of Royal Society B 324: 247 - 265.

Freer-Smith, P.H., Beckett, K.P., Taylor, G., 2005, Deposition velocities to *Sorbus aria*, *Acer campestre*, *Populus deltoides x trichocarpa* 'Beaupre', *Pinus nigra* and x *Cupressocyparis leylandii* for coarse, fine and ultra-fine particles in the urban environment. Environmental Pollution 133: 157 - 167.

Freer-Smith, P.H., El-Khatib, A.A., Taylor, G., 2004.Capture of Particulate Pollution by Trees: A Comparison of Species Typical of Semi-Arid Areas (*Ficus Nitida* and *Eucalyptus Globulus*) with European and North American Species. Water Air and Soil pollution. 155: 173 – 187.

Grote, R., Samson, R., Alonso, R., Amorim, J.H., Carinanos, P., Churkina, G., Fares, S., Thiec, D.L., Niinemets, U., Mikkelsen, T.N., Paoletti, E., Tiwary, A., Calfapietra, C., 2016. Functional traits of urban trees: air pollution mitigation potential. Frontiers in Ecology and the Environment 14: 543 – 550.

Gudesblat, G.E., Schneider-Pizon, J., Betti, C. 2012 SPEECHLESS integrated brassinosteroid and stomata signalling pathways. Nature Cell Biology 14: 548 - 54.

Hansard, R., Maher, B.A., Kinnersley.R., 2011. Biomagnetic monitoring of industry-derived particulate pollution. Environmental Pollution 159: 1673 – 1681.

Hofman, J., Maher, B.A., Muxworthy, A.R., Wuyts, K., Castanheiro, A., Samson, R., 2017. Biomagnetic monitoring of atmospheric pollution: a review of magnetic signatures from biological sensors. Environmental Science and Technology 51: 6648 - 6664.

Hofman, J., Stokkaer, I., Snauwaert, L., Samson, R., 2013. Spatial distribution assessment of particulate matter in an urban street canyon using biomagnetic leaf monitoring of tree crown deposited particles. Environmental pollution 183: 123 - 32.

Hofman, J., Wuyts, K., Van Wittenberghe, S., Brackx, M., Samson, R., 2014. On the link between biomagnetic monitoring and leaf-deposited dust load of urban trees: Relationships and spatial variability of different particle size fractions. Environmental Pollution 189: 63 - 72.

Holder, C.D., 2012. The relationship between leaf hydrophobicity, water droplet retention, and leaf angle of common species in a semi-arid region of western United States. Agricultural and Forest Meteorology 152: 11 – 16.

Hothorn, T., Hornik, K., Zeileis, A., 2006. Unbiased Recursive Partitioning: A Conditional Inference Framework. Journal of Computational and Graphical Statistics 15: 651 - 674.

Innes, J.L., 1985. Lichenometry. Progress in Physical Geography 9:187-254.

Jordanova, D., Petrov, P., Hoffmann, V., Gocht, T., Panaiotu, C., Tsacheva, T., Jordanova, N., 2010. Magnetic signature of different vegetation species in polluted environment. Studia Geophysica et Geodaetica 54: 417 - 442.

Kardel, F., Wuyts, K., Babanezhad, M., Vitharana, U.W.A., Wuytack, T., Potters, G., Samson, R., 2010. Assessing urban habitat quality based on specific leaf area and stomatal characteristics of Plantago lanceolata L. Environmental Pollution 158: 788 - 794.

Kardel, F., Wuyts, K., Babanezhad, M., Wuytack, T., Adriaenssens, S., Samson, R., 2012. Tree leaf wettability as passive bio indicator of urban habitat quality. Environmental and Experimental Botany 75: 277 - 285.

Kardel, F., Wuyts, K., Maher, B.A., Hansard, R., Samson, R., 2011. Leaf saturation isothermal remanent magnetization (SIRM) as a proxy for particulate matter monitoring: Inter-species differences and in season variation. Atmospheric Environment. 45: 5164 - 5171.

Larcher, W., 2003. Physiological Plant Ecology: Ecophysiology and Stress Physiology of Functional Groups, fourth ed. Springer, 48 - 53.

Lehndroff, E., Urbat, M., Schwark, L., 2006. Accumulation histories of magnetic particles on pine needles as function of air quality. Atmospheric Environment 40(36): 7082 – 7096.

Leonard, R.J., McArthur, C., Hochuli, D.F., 2016. Particulate matter deposition on roadside plants and the importance of leaf trait combinations. Urban Forestry and Urban Greening 20: 249 - 253.

Liaw, A., Wiener, M., 2002. Classification of regression by randomForest. R News 2, 18 – 22.

Matzka, J., Maher, B. A., 1999. Magnetic biomonitoring of roadside tree leaves: Identification of spatial and temporal variations in vehicle derived particles. Atmospheric Environment. 33: 4565 – 4569.

McIntosh, G., Gómez-Paccard, M., Osete, M.L., 2007. The magnetic properties of particles deposited on Platanus x hispanica leaves in Madrid, Spain, and their temporal and spatial variations. The Science of the Total Environment 382: 135 - 146.

McPherson, G., Simpson, J.R., Peper, P.J., Maco, S.E., Xiao, Q., 2005. Municipal forest benefits and costs in five US cities. Journal of Forestry 103: 411 – 416.

Mitchell, R., Maher, B.A., Kinnersley, R., 2010. Rates of particulate pollution deposition onto leaf surfaces: Temporal and interspecies magnetic analyses. Environmental Pollution 158: 1472-1478.

Moreno, E., Sagnotti, l., Dinares-Turell, J., Legzdins, A.E., Cascella, A., 2003. Biomonitoring of traffic air pollution in Rome using magnetic properties of tree leaves. Atmospheric Environment 37: 2967 - 2977.

Mori, J., Sæbø, A., Hanslin, H.M., Teani, A., Ferrini, F., Fini, A., Burchi, G., 2015. Deposition of traffic-related air pollutants on leaves of six evergreen shrub species during a Mediterranean summer season. Urban Forestry and Urban Greening 14: 264 - 273.

Nali, C., Lorenzini. G., 2007. Air quality survey carried out by school children: An innovative tool for urban planning. Environmental Monitoring and Assessment 131: 201-210.

Neinhuis, C., Barthlott, W., 1997. Characterization and distribution of water repellent, self-cleaning plant surfaces. Annals of Botany 79: 667 - 77.

Neinhuis, C., Barthlott, W., 1998. Seasonal changes of leaf surface contamination in beech, oak, and ginkgo in relation to leaf micromorphology and wettability. New Phytologist 138: 91 – 98.

Nicotra, A., Cosgrove, M., Cowling, A., Schlichting, C., Jones, C., 2008. Leaf shape linked to photosynthetic rates and temperature optima in South African Pelargonium species Oecologia 154: 625 - 635.

Nowak, D.J., Crane, D., Stevens, J., 2006. Air pollution removal by urban trees and shrubs in the United States. Urban Forestry and Urban Greening 4: 115 – 23.

Philibert, A., Loyce, C., Makowski, D., 2013. Prediction of N2O emission from local information with Random Forest. Environmental Pollution 177: 156 – 63.

Pomeranz, M., Campbell, J., Siegal-Gaskins, D., Engelmeier, J., Wilson, T., Fernandez, V., Brkljacic, J., Grotewold. E., 2013. High-resolution computational imaging of leaf hair patterning using polarized light microscopy. The Plant Journal 73: 701 - 708.

Poorter, H., Niinemets, Ü., Poorter. L., Wright, I., Villar, R., 2009. Causes and consequences of variation in leaf mass per area (LMA): a meta-analysis. New Phytologist 182: 565 - 588.

Popek, R., Gawrońska, H., Wrochna, M., Gawroński, S.W., Sæbø, A., 2013. Particulate matter on foliage of 13 woody species: Deposition on surfaces and phytostabilisation in waxes - a 3-year study. International Journal of Phytoremediation 15: 245 - 256.

Przybysz, A., Sæbø, A., Hanslin, H.M., Gawronski, S.W., 2014. Accumulation of particulate matter and trace elements on vegetation as affected by pollution level, rainfall and the passage of time. The Science of Total Environment 481: 360 - 69.

Rai, P.K., 2013. Environmental magnetic studies of particulates with special reference to biomagnetic monitoring using roadside plant leaves. Atmospheric Environment 72: 113 – 129

Räsänen, Janne V., Holopainen, T., Joutsensaari, J., Ndam, C., Pasanen, P., Rinnan, Å., Kivimäenpää, M., 2013. Effects of species-specific leaf characteristics and reduced water availability on fine particle capture efficiency of trees. Environmental Pollution 183: 64 - 70.

Russ, J.C., The Image Processing Handbook. 2002. Fourth ed. CRC Press. Chapter 9: Feature specific measurements

Sæbø, A., Popek, R., Nawrot, B., Hanslin, H.M., Gawronska, H., Gawronski, S.W., 2012. Plant species differences in particulate matter accumulation on leaf surfaces. Science of Total Environment 427-428: 347 - 354.

Song, Y., Maher, B.A., Li, F., Wang, X., Sun, X., Zhang, H. 2015. Particulate matter deposited on leaf of five evergreen species in Beijing, China: Source identification and size distribution. Atmospheric Environment 105: 53 - 60.

Stalder, AF., Kulik, G., Sage, D., Barbieri, L., Hoffmann, P., 2006. A snake-based approach to accurate determination of both contact points and contact angles. Colliodes and surfaces A: physicochem. Engineering aspects 286: 92 - 103.

Suzuki, K., 2006, Characterisation of airborne particulates and associated trace metals deposited on tree bark by ICP-OES, ICP-MS, SEM-EDX, and laser ablation ICP-MS. Atmospheric Environment 40: 2626 - 2634.

Van der Waal, R., Bonn, A., Monteith, D., Reed, M., Blackstock, K., Hanley, N., Thompson, D., Evans, M., Alonso, I., Allott, T., Armitage, H., Beharry, N., Glass, J., Johnson, S., McMorrow, J., Ross, L., Pakemane, R., Perry, S., Tinch, D., 2011. Mountains, Moorlands and Heaths. Chapter 5 (UK National Ecosystem Assessment: technical report). , pp. 105–160 (pp)

Weerakkody, U., Dover, J. W., Mitchell, P., Reiling, K., 2018. Evaluating the impact of individual leaf traits on atmospheric particulate matter accumulation using natural and synthetic leaves. Urban Forestry and Urban Greening 30: 98 - 107.

WHO, Working Group, 2006, Health risks of particulate matter from long-range transboundary air pollution. European Centre for Environment and Health, Bonn. World Health Organization.

Wright, I.J., Reich, P.B., Westoby, M., Ackerly, D.D., Baruch, Z., Bongers, F., Cavender-Bares, J., Chapin, T., Cornelissen, J.H.C., Diemer, M., 2004. The worldwide leaf economics spectrum. Nature. 428: 821 - 827.

Wuytack, T., Wuyts, K., Van Dongen, S., Baeten, L., Kardel, F., Verheyen, K., Samson, R., 2011. The effect of air pollution and other environmental stressors on leaf fluctuating asymmetry and specific leaf area of *Salix alba* L. Environmental Pollution. 159: 2405-2411.

Table 1

Overview of the data subsets used for ® randomForest (RF) built according to the functional plant types and time period considered. N = number of plant species included. Observations = number of observations included in the RF model. Model "AS" - all plant species (n = 96) in September. "BJ" – deciduous needle-like and broadleaves for June. "BS"- deciduous needle-like and broadleaves for September. "BD" Difference (∆) in leaf SIRM between June and September for deciduous broadleaves. "EJ"- evergreen: needle/scale-like, broadleaves, and climber species for June. "ES"- evergreen: needle/scale-like, broadleaves, and climber species for September. "AS-SD"- plant species accounted for stomatal density in September. "DEBS-TD" deciduous and evergreen broadleaf plant species with trichome density in September. "DEBD-TD" – deciduous and evergreen broadleaf plant species with trichome density with the difference in leaf SIRM between June and September.

Model	Type	Time period	N	Observations
AS	All species	September	96	466
BJ	Deciduous needle-like and broadleaves	June	77	364
BS	Deciduous needle-like and broadleaves	September	77	364
BD	Deciduous needle-like and broadleaves	∆ June – September	77	364
EJ	Evergreen (needle-like/ broadleaves)	June	19	98
ES	Evergreen (needle-like/ broadleaves)	September	19	103
AS-SD	All species with SD data	September	38	187
DEBS-TD	All broadleaves with TD data	September	51	247
DEBD-TD	All broadleaves with TD data	∆ June – September	51	247

Table 2

Analyzed plant species (n = 96) with indication of family (n = 29) denoted as (1 - 29) # see text box below and plant type (n = 5, C = conifer, E.B = evergreen broadleaf, T = deciduous tree, S = deciduous shrub, CL = climber) with clusters (n = 5) based on morphological and anatomical leaf traits– Single leaf area (LA cm^2) specific leaf area (SLA m^2 $kg^{-}1$), leaf dissection index (LDI dimensionless), leaf roundness (dimensionless) drop contact angle (DCA °) at abaxial (AB) and adaxial (AD) leaf side Saturation Isothermal Remanent Magnetization (SIRM µA). Stomatal density (mm^{-2}) and trichome density (mm^{-2}), trichome presence "N" = No, "Y" = Yes, "+++" dense fibrous network of trichomes - trichome density not measured, "n/a" trichomes present but not captured in the sample due to sparse presence. Leaves of plant species names in the bold text are one year old in June 2016 and have missing leaf SIRM values indicated by a hyphen "-".

		JUNE							SEPTEMBER									
SPECIES	CLUSTER	LA	SLA	LDI	ROUNDNESS	DCA (AB)	DCA (AD)	SIRM	LA	SLA	LDI	ROUNDNESS	DCA (AB)	DCA (AD)	SIRM	STOMATAL DENSITY	TRICHOME PRESENCE	TRICHOME DENSITY
Abies fraseri **(C)** [21]	3	0.26	3.34	16.54	0.12	73	72	-	0.10	6.00	12.77	0.09	90	56	11.68	122.4	N	0.00
Abies koreana **(C)** [21]	3	0.28	3.31	15.20	0.14	115	89	-	0.36	5.88	12.65	0.14	111	66	10.49	131.5	N	0.00
Abies nordmanniana **(C)** [21]	3	0.45	3.31	16.99	0.10	72	68	-	0.45	5.34	15.99	0.10	64	64	10.28	104.2	N	0.00
Acer campestre (T) [26]	4	27.14	14.79	11.52	0.86	69	83	7.91	28.04	13.39	14.09	0.90	67	78	28.88	0.0	Y	4.04
Acer ginnala (T) [26]	2	30.52	18.31	10.67	0.83	88	81	3.99	28.35	13.70	9.99	0.78	61	73	14.47	628.1	N	0.00
Acer platanoides (T) [26]	4	87.05	19.70	13.43	0.85	86	96	5.58	71.82	14.28	13.97	0.78	76	67	20.96	0.0	Y	n/a
Acer pseudoplatanus (T) [26]	5	113.28	15.98	11.87	0.78	133	76	6.46	96.95	13.39	15.22	0.94	106	63	9.07	0.0	N	0.00
Aesculus hippocastanum (T) [26]	4	85.52	13.15	8.89	0.47	97	84	6.80	65.01	9.91	9.36	0.45	88	62	29.59	0.0	Y	9.96
Alnus glutinosa (T) [6]	4	43.62	16.42	7.59	0.90	65	65	8.15	48.59	18.85	7.40	0.82	59	58	9.00	0.0	Y	0.46
Alnus incana (T) [6]	5	38.84	19.48	7.90	0.83	115	75	5.27	50.26	13.76	7.81	0.79	98	69	20.43	0.0	Y	9.00
Amelanchier lamarckii (S) [24]	2	22.70	18.54	8.04	0.57	113	85	3.71	24.50	13.49	8.12	0.65	77	85	17.55	97.9	N	0.00
Betula pendula (T) [6]	4	14.71	22.20	9.63	0.79	73	75	3.53	22.17	14.48	9.89	0.89	76	74	10.35	0.0	Y	n/a
Buddleja davidii (S) [27]	1	33.46	12.17	11.84	0.49	133	76	6.41	32.49	10.29	8.80	0.47	124	63	37.97	0.0	Y	+++
Carpinus betulus (T) [6]	4	14.85	18.54	8.74	0.57	89	76	6.32	25.16	14.22	8.71	0.62	67	74	30.95	0.0	Y	1.17
Castanea sativa (T) [15]	4	65.12	16.55	10.88	0.35	68	73	6.02	68.04	10.99	12.36	0.31	64	70	15.72	0.0	Y	13.58
Catalpa bignonioides (T) [7]	2	64.77	25.43	7.52	0.73	94	79	3.70	171.89	16.37	8.00	0.87	80	62	9.73	422.1	Y	5.29
Cedrus deodara **(C)** [21]	3	0.64	2.42	25.99	0.03	96	101	-	0.18	3.83	26.40	0.05	71	79	12.77	155.3	N	0.00
Chamaecyparis lawsoniana **(C)** [11]	3	27.86	4.58	41.85	0.46	111	117	-	61.09	8.04	42.50	0.56	108	104	12.59	0.0	N	0.00
Cornus alba (S) [10]	5	38.69	22.13	7.28	0.55	120	88	3.80	50.80	17.23	7.93	0.63	111	73	11.13	0.0	Y	21.54
Cornus mas (T) [10]	4	21.60	15.36	7.15	0.64	78	83	4.86	25.01	10.38	7.67	0.64	62	74	11.00	0.0	Y	5.96
Cornus sanguinea (S) [10]	4	30.14	19.15	7.09	0.85	81	74	3.16	43.94	13.29	8.03	0.78	63	74	12.84	0.0	Y	15.63
Corylus avellana (S) [6]	4	61.17	17.34	8.98	0.87	77	76	6.37	77.53	16.05	9.47	0.84	63	69	20.27	0.0	Y	4.38
Corylus colurna (T) [6]	4	20.65	20.70	9.28	0.81	62	56	8.18	72.90	15.48	8.29	0.91	57	63	20.43	0.0	Y	9.50
Crataegus monogyna (T) [24]	4	14.07	17.12	10.97	0.92	98	78	3.81	12.34	10.62	13.20	0.95	72	65	16.15	0.0	Y	1.08
Elaeagnus angustifolia (T) [12]	5	7.28	18.35	8.13	0.30	147	85	8.11	10.13	20.16	7.93	0.42	124	79	14.12	0.0	Y	45.13
Euonymus europaeus (S) [9]	4	18.65	14.63	7.97	0.53	88	88	4.99	27.16	13.22	7.96	0.60	63	74	15.24	0.0	Y	n/a
Fagus sylvatica (T) [15]	4	12.59	19.00	7.18	0.62	92	90	8.55	11.78	17.27	7.37	0.60	69	75	22.07	0.0	Y	9.67
Fraxinus excelsior (T) [20]	4	14.25	15.90	8.31	0.48	71	80	4.34	23.23	12.94	9.47	0.46	55	64	14.44	0.0	Y	n/a

SPECIES	CLUSTER	JUNE							SEPTEMBER							STOMATAL DENSITY	TRICHOME PRESENCE	TRICHOME DENSITY
		LA	SLA	LDI	ROUNDNESS	DCA (AB)	DCA (AD)	SIRM	LA	SLA	LDI	ROUNDNESS	DCA (AB)	DCA (AD)	SIRM			
Fraxinus ornus (T) [20]	2	15.88	16.16	8.27	0.48	80	67	4.05	14.17	11.90	9.73	0.57	67	67	12.46	222.9	N	0.00
Ginkgo biloba (T) [16]	5	22.78	11.77	9.80	0.74	131	127	3.14	27.41	8.75	10.83	0.66	117	70	12.89	56.9	N	0.00
***Hedera helix* (CL)** [3]	4	30.79	11.60	6.99	0.80	74	82	-	23.38	11.71	7.87	0.80	72	74	9.09	0.0	Y	0.58
Hibiscus syriacus (S) [19]	2	15.38	22.33	8.18	0.76	77	73	3.90	21.03	15.18	9.49	0.66	60	62	14.60	342.9	Y	1.29
Hippophae rhamnoides (S) [12]	5	2.26	11.87	11.89	0.12	117	86	7.11	2.75	11.80	13.47	0.12	101	84	16.11	0.0	N	0.00
***Ilex aquifolium* (E.B)** [4]	2	13.13	6.98	12.31	0.41	93	89	-	15.98	6.53	12.33	0.53	80	83	9.54	192.9	N	0.00
Juglans regia (T) [17]	2	49.52	19.74	7.52	0.53	76	71	3.26	56.72	12.31	7.58	0.57	60	69	17.33	220.1	N	0.00
***Juniperus communis* (C)** [11]	3	0.20	3.50	13.45	0.11	99	89	-	0.19	4.69	15.06	0.10	81	72	18.59	19.2	N	0.00
Laburnum anagyroides (T) [14]	5	12.50	15.57	8.26	0.48	133	113	2.41	16.83	14.47	8.10	0.48	115	76	13.02	0.0	Y	11.13
Larix decidua (C) [21]	3	0.22	8.29	19.11	0.07	114	105	6.58	0.29	8.71	22.41	0.08	84	76	8.39	150.7	N	0.00
Larix kaempferi (C) [21]	3	0.19	6.00	17.57	0.07	111	112	5.95	0.54	10.39	25.79	0.11	101	87	7.29	0.0	N	0.00
Ligustrum ovalifolium (S) [20]	2	9.98	11.56	7.64	0.54	85	79	4.52	21.14	9.50	7.95	0.48	60	71	13.37	417.0	N	0.00
Ligustrum vulgare (S) [20]	2	5.35	13.95	7.86	0.36	95	98	5.51	11.46	10.17	8.23	0.34	85	74	12.94	203.3	N	0.00
Liquidambar styraciflua (T) [2]	2	20.31	21.54	10.30	0.86	98	98	3.61	46.60	15.29	14.16	0.92	83	67	7.88	183.5	N	0.00
Liriodendron tulipifera (T) [18]	5	54.62	24.06	9.22	0.88	135	133	2.44	182.28	21.97	11.62	0.82	125	93	7.80	166.7	N	0.00
***Lonicera periclymenum* (CL)** [8]	5	15.14	19.21	7.06	0.70	134	123	-	23.77	16.67	7.38	0.74	105	93	9.83	212.0	Y	3.92
Lonicera tatarica (S) [8]	5	10.65	14.32	6.89	0.74	137	136	3.74	11.62	10.39	6.80	0.82	112	58	17.30	156.8	N	0.00
Lonicera xylosteum (S) [8]	5	14.32	18.30	7.06	0.68	140	134	3.62	18.92	13.86	7.00	0.60	112	69	19.70	0.0	Y	8.83
Magnolia kobus (T) [20]	2	41.89	20.82	7.77	0.44	101	104	4.89	48.09	18.56	8.76	0.48	77	64	12.83	226.8	Y	5.75
***Mahonia aquifolium* (E.B)** [5]	2	9.93	14.31	7.77	0.50	132	86	-	21.99	9.38	8.30	0.59	89	69	12.42	302.1	N	0.00
Malus sylvestris (T) [24]	1	24.04	18.34	8.25	0.56	93	81	7.33	29.54	14.02	9.00	0.69	87	76	12.62	0.0	Y	+++
Mespilus germanica (T) [24]	4	22.15	14.96	7.80	0.48	92	85	7.91	18.58	10.21	8.15	0.47	71	74	22.70	0.0	Y	21.33
***Picea abies* (C)** [21]	3	0.19	4.01	19.39	0.07	100	104	-	0.20	5.64	18.46	0.09	66	82	11.78	187.9	N	0.00
***Picea pungens glauca* (C)** [21]	3	0.26	3.44	16.24	0.10	80	82	-	0.30	3.84	16.87	0.09	88	93	17.97	183.3	N	0.00
***Pinus nigra* (C)** [21]	3	1.30	6.62	29.09	0.09	76	86	-	1.10	4.61	33.02	0.05	75	77	12.30	168.1	N	0.00
Platanus × acerifolia (T) [22]	4	101.59	21.20	9.18	0.85	99	83	4.92	90.00	16.66	12.05	0.84	55	80	7.01	0.0	Y	2.08
Populus alba (T) [25]	4	53.48	19.78	8.79	0.83	93	85	2.40	61.48	20.64	8.39	0.81	75	76	3.08	0.0	Y	n/a
Prunus avium (T) [24]	2	40.36	21.67	8.37	0.56	87	86	5.39	40.97	14.50	8.90	0.57	74	64	17.88	348.6	Y	3.17
***Prunus laurocerasus* (E.B)** [24]	2	38.30	9.90	7.57	0.52	85	85	-	48.46	7.83	10.05	0.49	81	78	9.60	179.3	N	0.00
Prunus padus (S) [24]	5	30.62	15.59	8.34	0.53	126	92	5.89	53.22	11.21	8.52	0.53	96	69	18.15	0.0	Y	0.13
Prunus spinosa (S) [24]	4	7.02	13.86	7.05	0.63	100	86	7.07	10.96	9.92	7.98	0.60	82	66	20.33	0.0	Y	8.17
***Pseudotsuga menziesii* (C)** [21]	3	0.34	5.29	18.2	0.08	90	84	-	0.15	6.63	18.34	0.05	91	76	21.05	143.8	N	0.00
***Quercus ilex* (E.B)** [15]	1	19.55	8.52	7.64	0.56	130	71	-	10.07	6.83	8.06	0.49	100	66	24.08	0.0	Y	+++
Quercus palustris (T) [15]	2	26.80	17.53	13.7	0.38	99	87	5.56	23.91	16.98	14.52	0.41	57	65	8.48	428.8	N	0.00
Quercus petraea (T) [15]	2	16.29	14.24	9.79	0.58	133	93	5.93	27.07	12.39	10.62	0.48	110	75	22.10	551.0	Y	13.38

SPECIES	CLUSTER	JUNE							SEPTEMBER									
		LA	SLA	LDI	ROUNDNESS	DCA (AB)	DCA (AD)	SIRM	LA	SLA	LDI	ROUNDNESS	DCA (AB)	DCA (AD)	SIRM	STOMATAL DENSITY	TRICHOME PRESENCE	TRICHOME DENSITY
Quercus robur (T) [15]	2	19.02	16.94	12.55	0.49	131	119	4.26	25.32	13.08	11.73	0.54	94	80	21.89	446.7	N	0.00
Quercus rubra (T) [15]	5	62.57	15.95	12.29	0.61	122	104	5.36	59.32	12.48	13.14	0.45	76	75	14.67	0.0	Y	n/a
Rhamnus cathartica (S) [23]	2	11.85	17.63	8.02	0.57	84	68	8.41	27.21	12.60	7.81	0.62	76	68	16.60	236.5	Y	1.17
Rhamnus frangula (S) [23]	2	15.58	21.31	7.25	0.63	91	83	4.98	19.26	16.15	7.79	0.57	62	71	20.16	406.2	N	0.00
***Rhododendron* (E.B)** [13]	2	27.68	10.16	8.08	0.35	58	76	-	46.74	6.48	8.63	0.35	55	59	15.06	255.5	N	0.00
Robinia pseudoacacia (T) [14]	5	8.24	28.26	7.18	0.70	141	132	1.71	10.50	23.59	7.31	0.49	125	123	4.41	0.0	Y	31.79
Rosa canina (S) [24]	2	4.74	16.82	7.97	0.67	97	123	5.66	4.46	14.44	9.29	0.62	89	103	9.22	131.8	N	0.00
Rosa glauca (S) [24]	5	5.87	17.92	8.78	0.67	131	129	3.14	6.39	13.89	8.13	0.53	126	124	7.77	84.0	N	0.00
Rosa pimpinellifolia (S) [24]	5	1.93	19.45	7.81	0.63	128	128	5.00	2.60	11.74	8.68	0.58	90	80	16.91	0.0	Y	n/a
Rosa rubiginosa (S) [24]	4	4.85	15.73	7.55	0.75	69	89	7.31	4.82	10.74	7.83	0.72	59	66	24.61	0.0	Y	9.88
Rosa rugosa (S) [24]	5	8.07	17.29	7.64	0.67	124	81	5.76	10.59	8.33	7.39	0.57	100	58	28.90	0.0	Y	28.88
Salix alba (T) [25]	5	9.42	17.40	8.93	0.27	125	74	3.78	17.01	11.89	11.12	0.26	110	67	14.68	0.0	Y	19.83
Salix aurita (S) [25]	5	5.48	20.44	7.50	0.75	134	120	4.60	9.64	14.38	7.51	0.68	126	68	22.80	0.0	Y	16.21
Salix caprea (T) [25]	5	19.09	22.42	7.67	0.67	133	71	4.74	36.82	16.34	8.00	0.74	125	64	12.27	0.0	Y	11.13
Salix cinerea (S) [25]	5	11.31	22.76	8.05	0.42	130	85	4.95	20.48	16.44	8.80	0.34	124	83	18.72	0.0	Y	20.46
Salix purpurea (S) [25]	2	4.86	19.69	9.13	0.35	130	132	1.34	12.05	14.72	11.31	0.19	121	112	8.07	735.9	N	0.00
Salix repens (S) [25]	5	1.59	14.89	7.31	0.47	129	69	6.00	4.62	12.31	7.67	0.55	123	81	21.89	0.0	Y	38.42
Salix rosmarinifolia (S) [25]	1	3.81	13.89	16.46	0.08	137	69	5.18	4.96	9.89	15.84	0.08	128	78	17.71	0.0	Y	+++
Salix viminalis (S) [25]	5	17.83	18.49	11.45	0.16	130	85	5.53	15.60	18.90	11.58	0.14	128	84	15.78	0.0	Y	16.96
Sambucus nigra (S) [1]	4	30.66	18.22	9.70	0.50	56	64	4.92	33.66	17.70	10.77	0.52	54	64	15.58	0.0	Y	1.38
Sorbus aria (T) [24]	1	25.12	16.53	9.12	0.75	139	82	7.36	43.12	11.37	9.26	0.64	130	61	30.21	0.0	Y	+++
Sorbus aucuparia (T) [24]	5	5.38	15.49	10.46	0.33	131	78	10.13	8.88	12.03	10.36	0.31	86	75	17.47	0.0	Y	3.29
Sorbus intermedia (T) [24]	1	30.87	11.10	10.37	0.55	135	79	13.87	40.89	7.87	12.08	0.53	110	63	23.53	0.0	Y	+++
Sorbus torminalis (T) [24]	4	50.64	13.09	11.76	0.83	84	77	5.12	40.43	11.23	11.52	0.80	61	59	13.49	0.0	Y	10.46
Symphoricarpos × chenaultii (S) [8]	5	3.11	13.59	7.14	0.62	140	135	4.34	2.90	13.72	7.27	0.72	126	92	12.70	0.0	Y	19.46
Syringa vulgaris (S) [20]	4	30.48	9.02	7.30	0.69	56	79	4.59	39.06	8.63	7.72	0.65	56	63	15.59	0.0	N	0.00
***Taxus baccata* (C)** [28]	2	0.46	7.10	10.93	0.13	94	75	-	0.46	6.78	11.88	0.12	86	66	11.69	94.5	N	0.00
***Thuja plicata* (C)** [11]	3	58.58	4.83	26.95	0.65	104	83	-	30.65	5.24	38.04	0.42	93	64	19.54	0.0	N	0.00
Tilia cordata (T) [19]	4	30.22	22.83	9.38	0.92	74	66	3.61	49.88	15.70	7.60	0.89	70	76	12.76	0.0	N	0.00
Tilia platyphyllos (T) [24]	4	38.78	23.31	8.21	0.85	84	59	5.61	82.97	15.11	8.71	0.88	61	59	21.39	0.0	Y	6.75
Ulmus glabra (T) [29]	4	34.43	17.19	8.87	0.66	85	85	6.12	68.01	12.28	9.52	0.87	67	55	27.06	0.0	Y	10.29
Viburnum lantana (S) [1]	4	36.77	12.86	7.39	0.80	79	76	15.74	40.78	10.07	7.75	0.69	58	71	39.77	0.0	Y	8.38
Viburnum opulus (S) [1]	4	37.42	17.88	11.57	0.89	95	74	5.40	59.53	11.65	9.87	0.87	77	71	31.01	0.0	Y	22.29

# **Plant families:**	1 = Adoxaceae	2 = Altingiaceae	3 = Apiaceae	4 = Aquifoliaceae
5 = Berberidaceae	6 = Betulaceae	7 = Bignoniaceae	8 = Caprifoliaceae	9 = Celastraceae
10 = Cornaceae	11 = Cupressaceae	12 = Elaeagnaceae	13 = Ericaceae	14 = Fabaceae
15 = Fagaceae	16 = Ginkgoaceae	17 = Juglandaceae	18 = Magnoliaceae	19 = Malvaceae
20 = Oleaceae	21 = Pinaceae	22 = Platanaceae	23 = Rhamnaceae	24 = Rosaceae
25 = Salicaceae	26 = Sapindaceae	27 = Scrophulariaceae	28 = Taxaceae	29 = Ulmaceae

Table 3

Results of multiple linear regression (MLR) on leaf SIRM in June (for deciduous conifers, broadleaf tree and shrub species), in September (for all selected plant species) indicating the effect of leaf traits: specific leaf area (SLA), drop contact angle (DCA) [abaxial (AB) adaxial (AD)], leaf dissection index (LDI), stomatal density (SD) trichome density (TD), and leaf roundness, showing the estimate, standard error (SE), and the p-values. The leaf SIRM in June and September was transformed ln(SIRM). Significant effects (p-value ≤ 0.05) are shown in bold.

SIRM	Variable	Estimate	SE	p-value
June	Intercept	3.062×10^{0}	3.272×10^{-1}	**< 0.001**
(n = 77)	SLA	-1.660×10^{-2}	1.377×10^{-2}	0.232
	leaf roundness	-2.957×10^{-1}	2.212×10^{-1}	0.185
	DCA (AB)	-4.071×10^{-3}	1.994×10^{-3}	**0.045**
	DCA (AD)	-9.089×10^{-3}	3.777×10^{-3}	**0.018**
	SD	-6.421×10^{-4}	2.440×10^{-4}	**0.011**
	TD	8.054×10^{-5}	3.812×10^{-5}	**0.032**
September	Intercept	23.926×10^{0}	3.380×10^{0}	**<0.001**
(n = 96)	SLA	$- 5.001 \times 10^{1}$	1.345×10^{-1}	**<0.001**
	DCA (AD)	-8.711×10^{-2}	4.367×10^{-2}	**0.049**
	TD	1.138×10^{-3}	4.563×10^{-4}	**0.016**

Table 4

Results of the post-hoc test following ANOVA for testing differences in the leaf SIRM between five clusters of selected plant species (n = 96) based on leaf traits (see Fig. 6 for an explanation of cluster codes) for the leaf SIRM in June and September. Significant differences (p-value ≤ 0.05) are shown in bold.

Cluster comparison	**June p- value**	**September p- value**
Cluster 2 – Cluster 1	0.636	**0.005**
Cluster 3 – Cluster 1	**<0.0001**	**0.007**
Cluster 4 – Cluster 1	0.803	0.289
Cluster 5 – Cluster 1	0.559	**0.016**
Cluster 3 – Cluster 2	**<0.0001**	0.999
Cluster 4 – Cluster 2	0.986	**0.055**
Cluster 5 – Cluster 2	0.999	0.956
Cluster 4 – Cluster 3	**<0.0001**	0.118
Cluster 5 – Cluster 3	**<0.0001**	0.952
Cluster 5 – Cluster 4	0.956	0.242

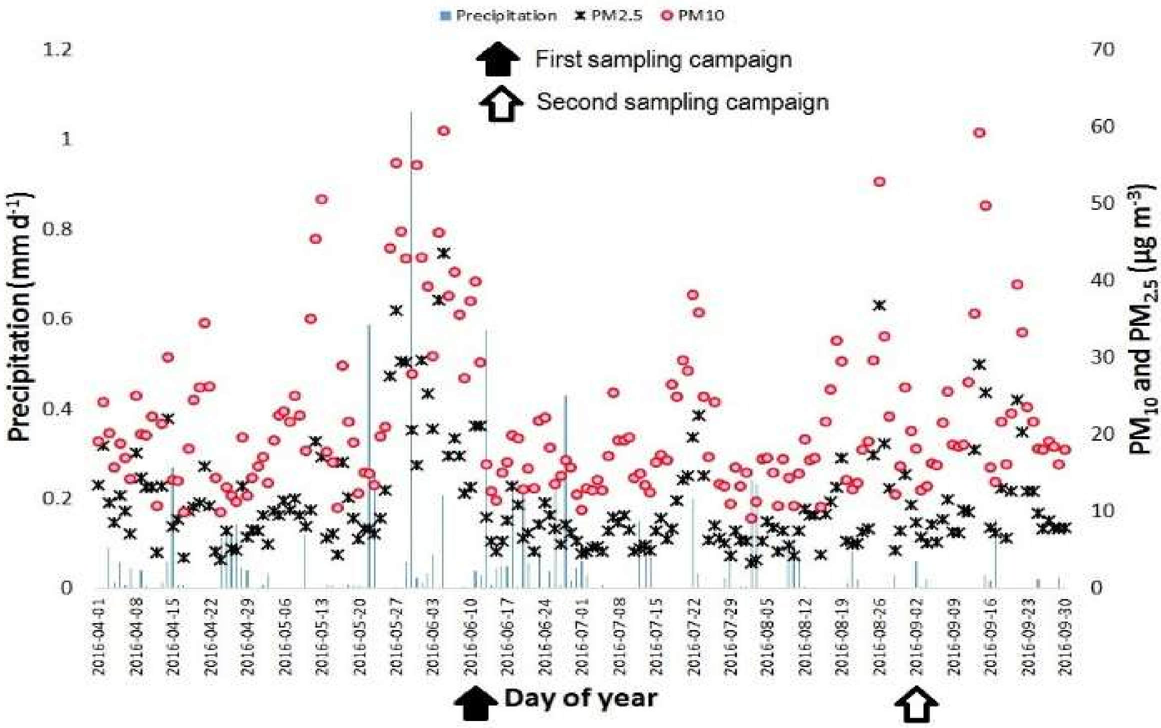

Fig. 1. Daily mean PM_{10} and $PM_{2.5}$ concentrations (µg m^{-3}) from the nearest monitoring station (42R817, Antwerpen, Groenenborgerlaan) and daily precipitation (mm d^{-1}) measured at Antwerpen Luchtbal (42M802 Havanstraat) illustrated from 1st April till 30th September 2016. First and second sampling campaign was organized on 9th to 10th June and 1st to 2nd September respectively. (Source: Flemish Environmental Agency, VMM).

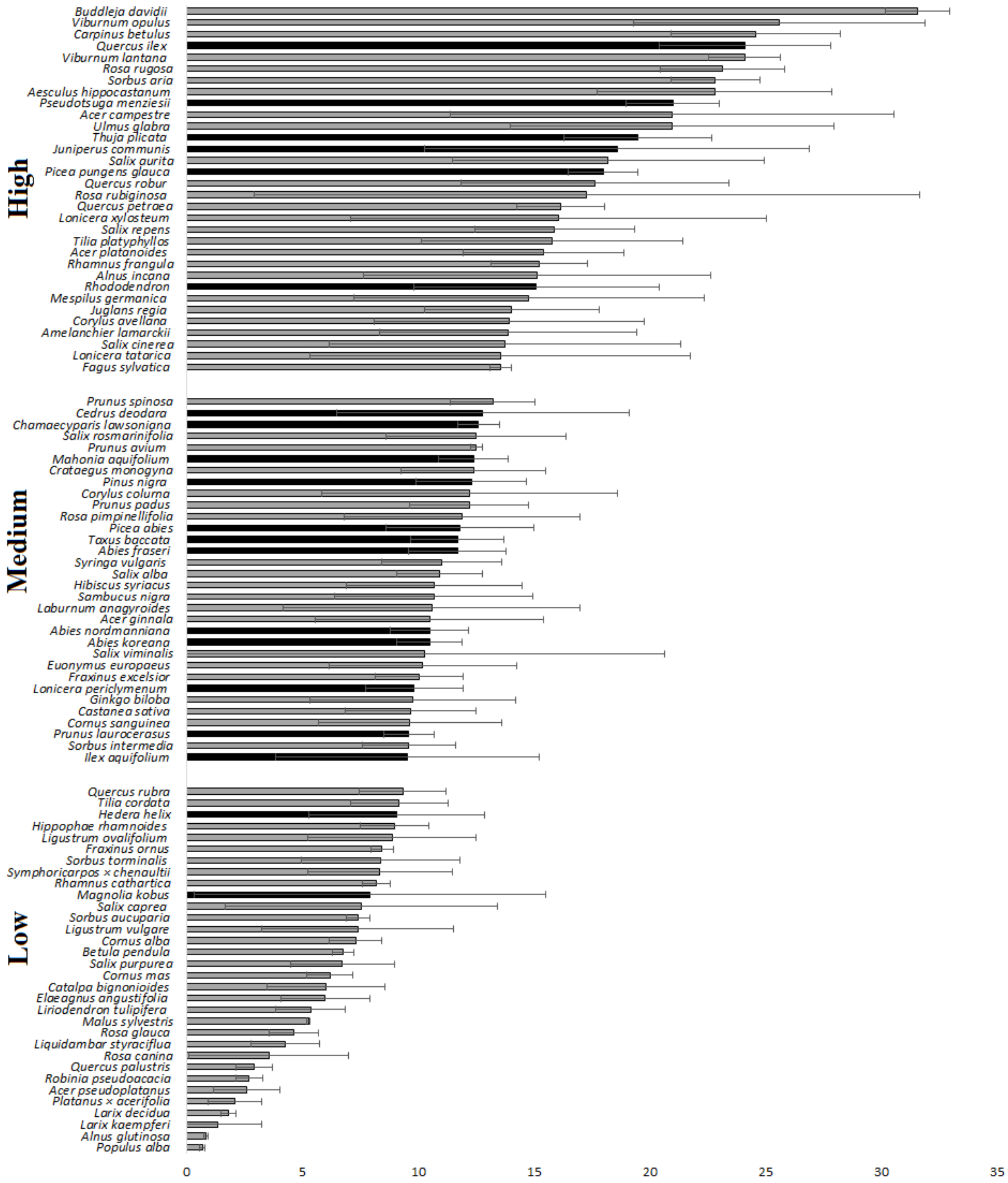

Fig. 2. Mean leaf area-normalized SIRM (μA) of selected urban plant species (n = 96) from a common garden in September 2016. Error bars are standard deviations. Gray bars – deciduous: conifers, broadleaf tree and shrub species, Black bars – evergreen: needle/scale-like, broadleaf and climber species. Note: Leaves of evergreen broadleaves, climbers and evergreen needle and scale-like conifers sampled in June were developed in the previous growing season and were about one year old in June. The leaf SIRM for investigated deciduous plant species is adjusted for equal exposure time by subtracting

the June leaf SIRM from September leaf SIRM. The leaf SIRM of needle/scale-like, evergreen broadleaves and climber species, was set to September leaf SIRM assuming the June leaf SIRM to be zero. Plant species grouped according to leaf SIRM into (low, medium, high) class using quantile classification.

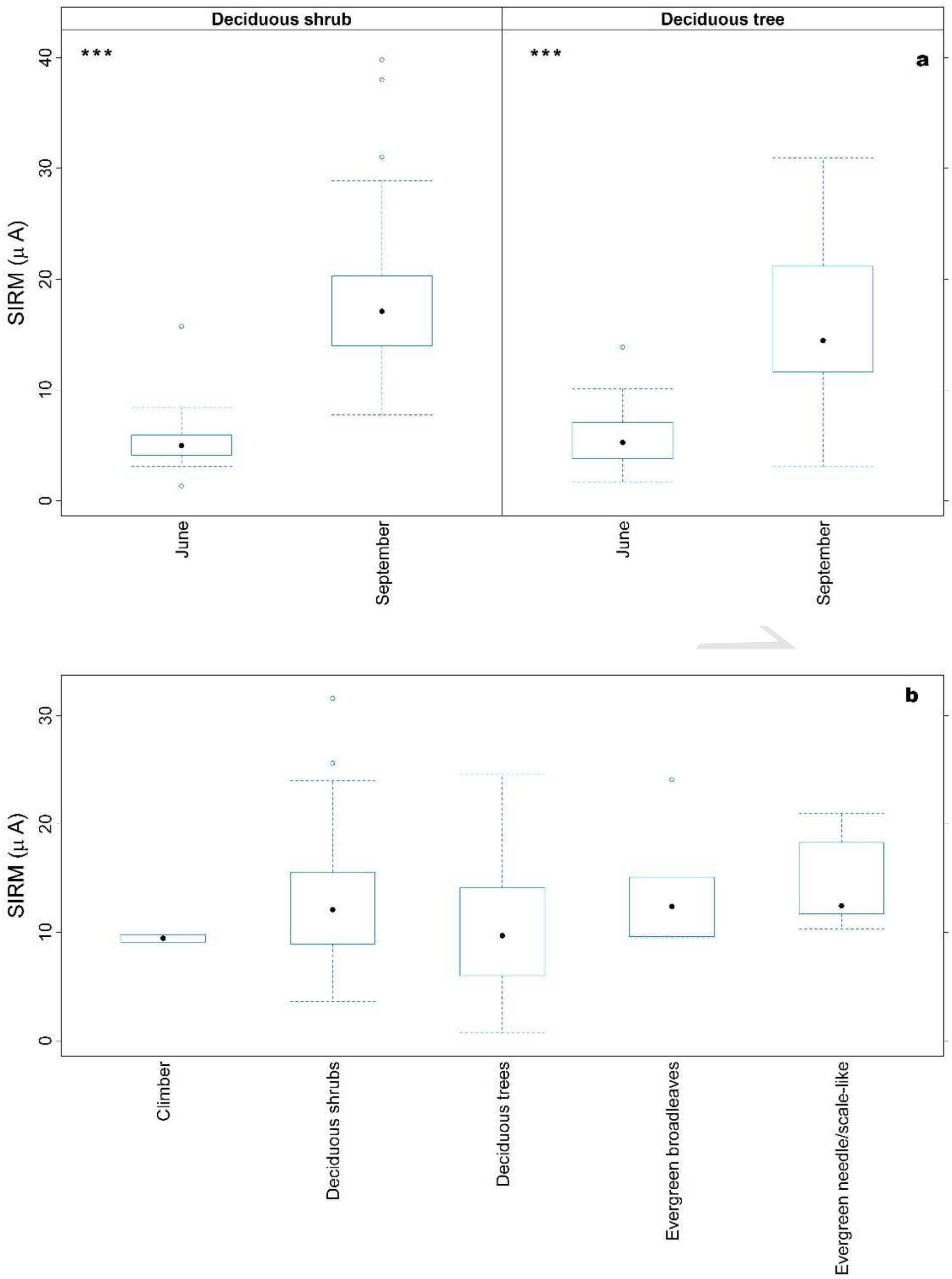

Fig. 3. (a) Box plots for leaf SIRM of deciduous needle-like and broadleaf trees (n = 45) and deciduous broadleaf shrubs (n = 32) in June and September. Results of paired sample t-tests of leaf SIRM between June and September are indicated by "***" p-value < 0.001. **(b)** Box plots for leaf SIRM of investigated plant types (n = 5) in September. For equal exposure time, the leaf SIRM of investigated deciduous plant species (n = 77) was adjusted by subtracting the June leaf SIRM from September leaf SIRM. The leaf SIRM of evergreen needle/scale-like, broadleaves and climber species was set to September leaf SIRM.

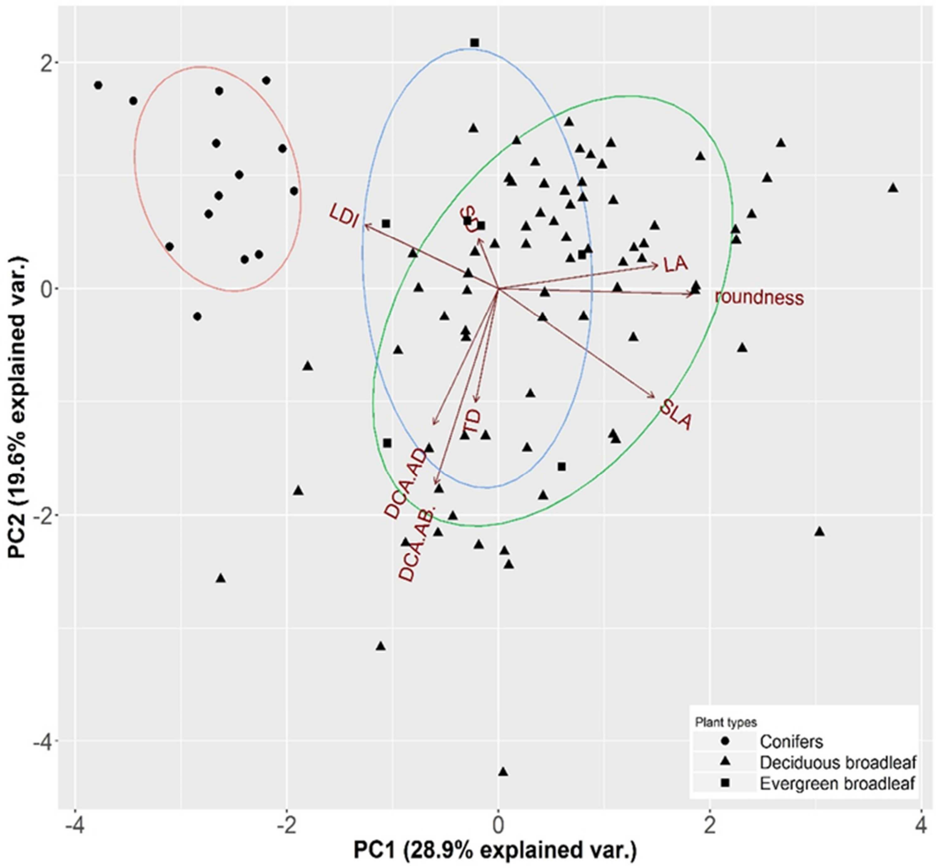

Fig. 4. Bi-plot of the principal component analysis on the anatomical and morphological variables measured at leaf level of the considered plant species (n = 96): leaf dissection index (LDI), leaf roundness (roundness), single leaf area (LA), specific leaf area (SLA), drop contact angle at abaxial (DCA AB), and adaxial (DCA AD), trichome density (TD), stomatal density (SD). Principal Component 1 (PC1) explains 28.9 %, and PC2 explains 19.6 % of the variance.

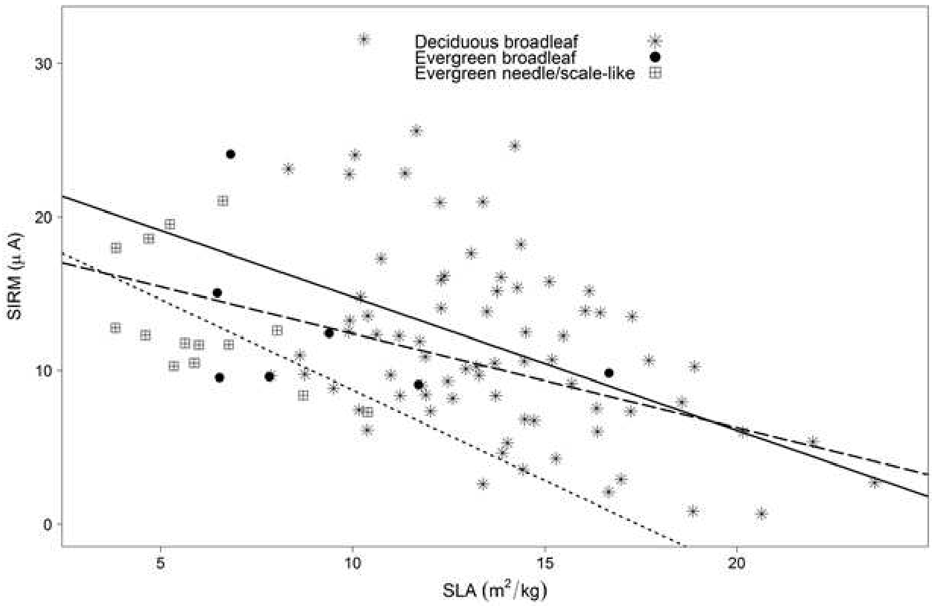

Fig. 5. SLA (m^2 /kg) in relation to leaf SIRM (µA) at species level for aggregated plant types (n = 3) Deciduous conifers, broadleaf consisting of trees and shrubs (n = 77, R^2 = 0.20, p < 0.001). Evergreen broadleaf including climber and evergreen broadleaves (n = 7, R^2 = 0.17, p = 0.344). Evergreen needle / scale-like conifers (n = 12, R^2 = 0.27, p = 0.051) in September 2016. Lines shown are regression lines – solid for deciduous broadleaf, dashed for evergreen broadleaf, dotted for evergreen needle/scale-like. SIRM values are re-calculated by subtracting the June leaf SIRM from the September leaf SIRM for all deciduous plant species. The leaf SIRM of evergreen (needle/scale-like, broadleaves and climber species), was set to the September leaf SIRM (see Table 2).

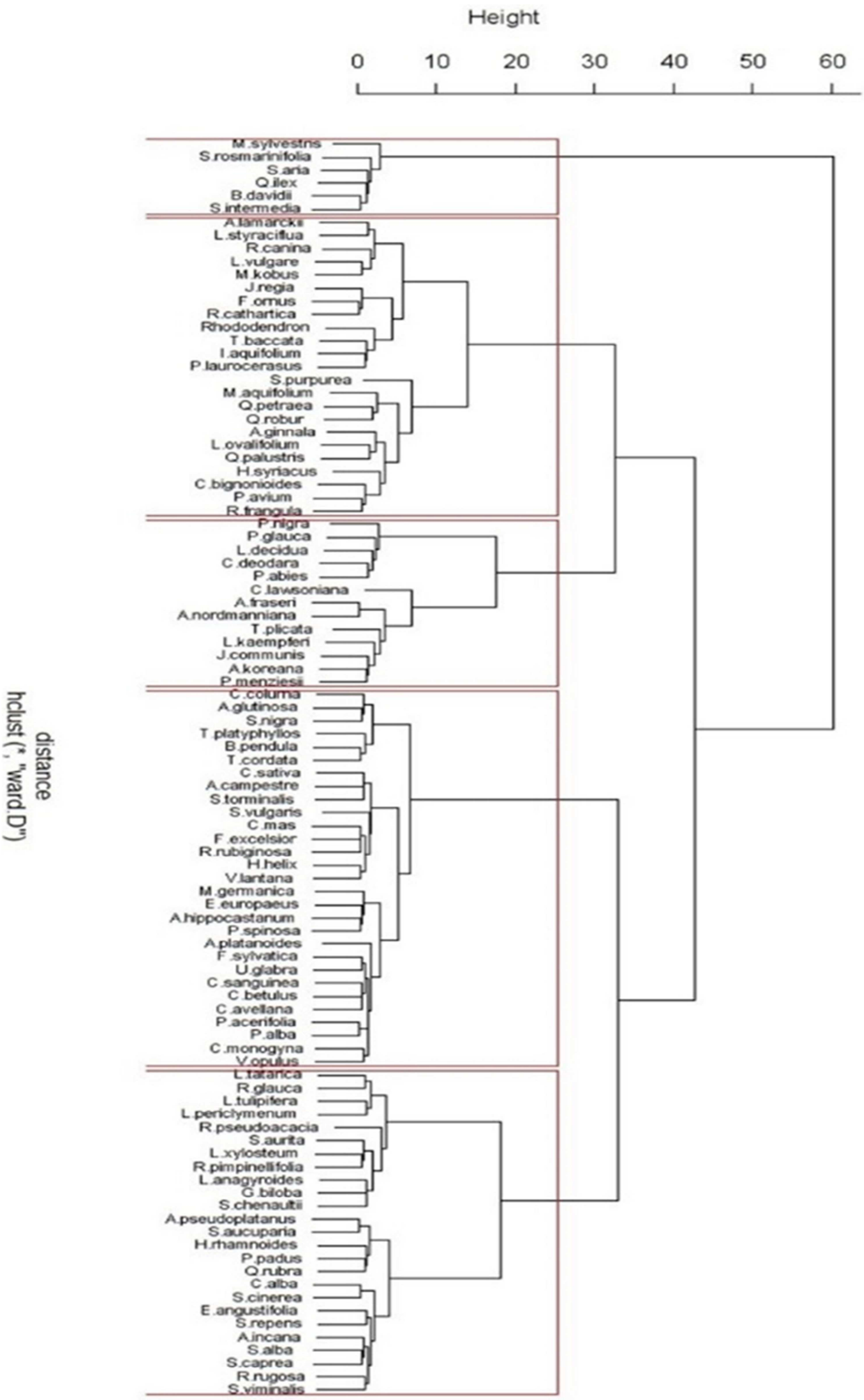

Fig. 6. Multivariate cluster analysis dendrogram in September using the Ward algorithm. Cluster 1 - 5 in order of appearance from top to bottom.

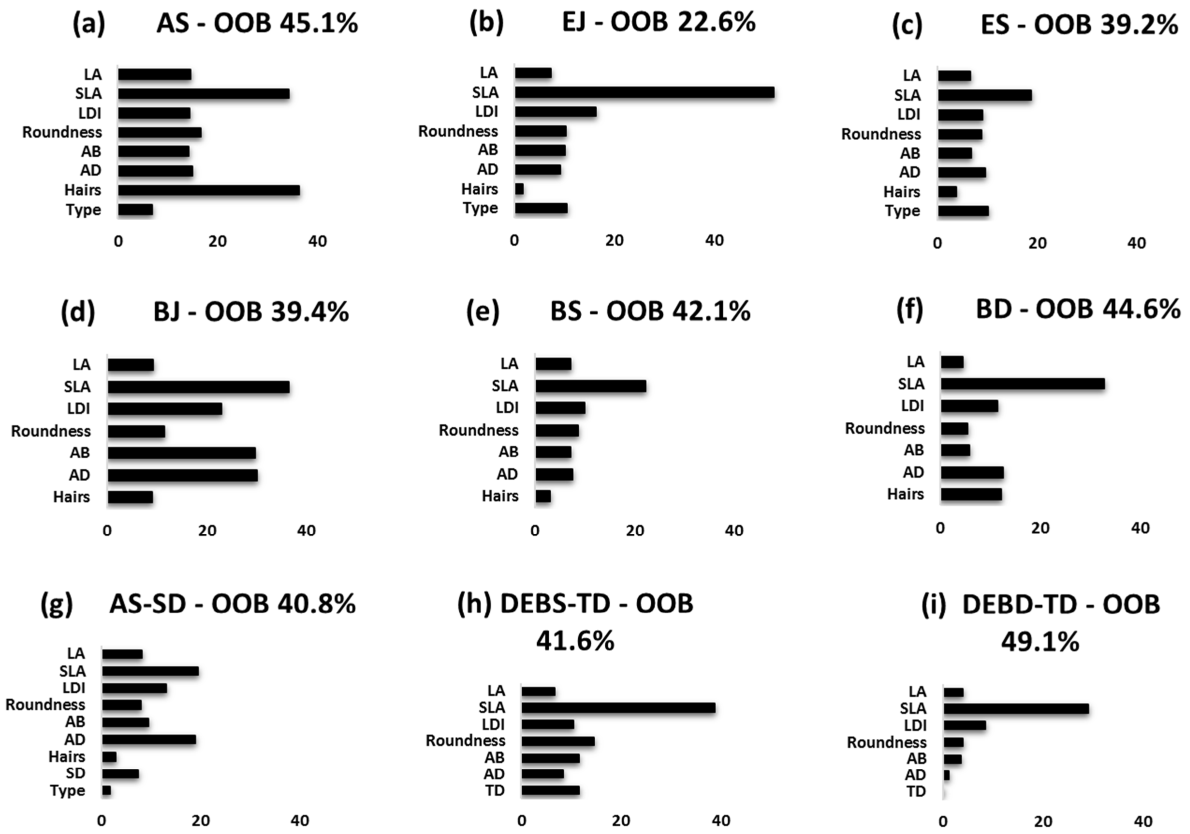

Fig. 7. Mean Decrease Accuracy (MDA) values are shown from 0 – 40 (Low value = less important, High value = more important) for the explanatory variables i.e. leaf area (LA), specific leaf area (SLA), leaf dissection index (LDI), leaf roundness, Drop contact angles – abaxial (AB) and adaxial (AD), presence of trichomes (Hairs), stomatal density (SD), trichome density (TD), type of leaf (needle, scale-like and broadleaves). The Out-of-bag error rate (OOB) for nine subsets of data (see Table 1) with leaf SIRM grouped as (low, medium, high) using quantile classification. (AS = all plant species in September, BJ = Broadleaves in June, EJ = evergreens in June, BS = Broadleaves in September, ES = evergreens in September, BD = ∆SIRM for broadleaves, AS-SD = species with SD data in September, DEBS-TD = deciduous /evergreen broadleaves species in September with TD data, DEBD- TD = deciduous /evergreen broadleaves species for ∆SIRM with TD data.

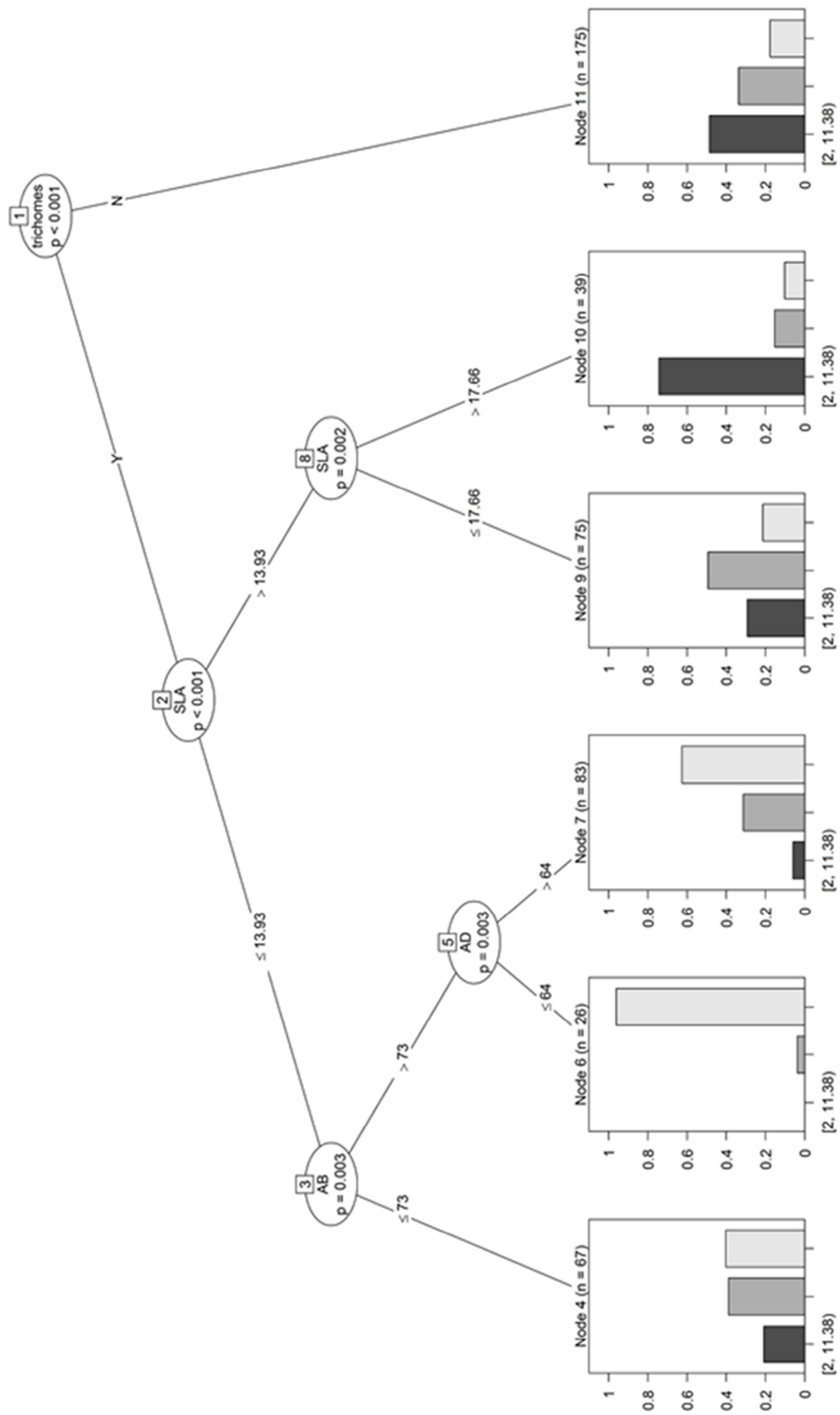
1
trichomes
p < 0.001
N
Y
2
SLA
p < 0.001
> 13.93
≤ 13.93
8
SLA
p = 0.002
> 17.66
≤ 17.66
3
AB
p = 0.003
≤ 73
> 73
5
AD
p = 0.003
≤ 64
> 64
Node 4 (n = 67)
Node 6 (n = 26)
Node 7 (n = 83)
Node 9 (n = 75)
Node 10 (n = 39)
Node 11 (n = 175)
1
0.8
0.6
0.4
0.2
0
[2, 11.38)

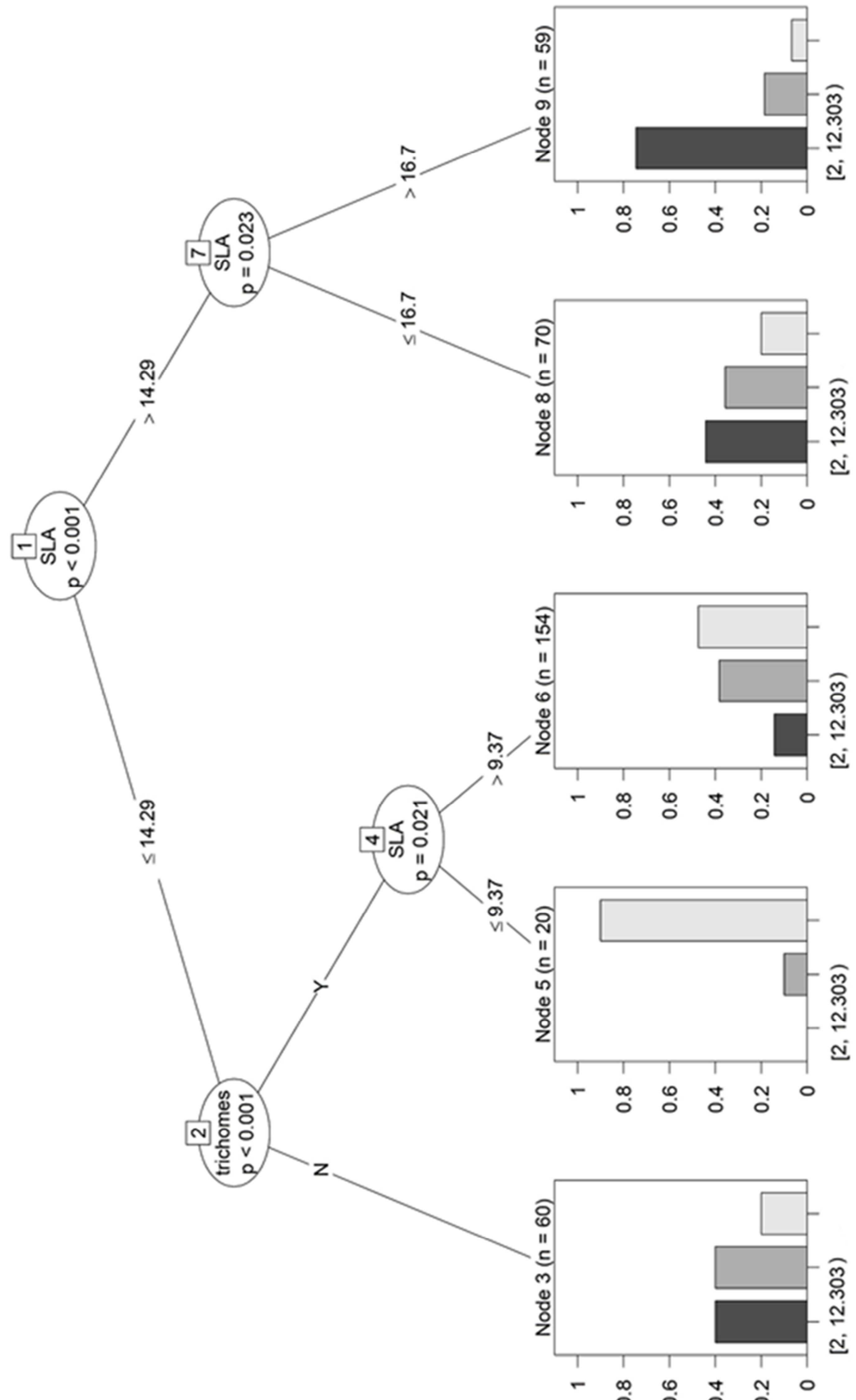
1
SLA
p < 0.001
≤ 14.29
> 14.29
2
trichomes
p < 0.001
N
Y
4
SLA
p = 0.021
≤ 9.37
> 9.37
7
SLA
p = 0.023
≤ 16.7
> 16.7
Node 3 (n = 60)
Node 5 (n = 20)
Node 6 (n = 154)
Node 8 (n = 70)
Node 9 (n = 59)
[2, 12.303)
1
0.8
0.6
0.4
0.2
0

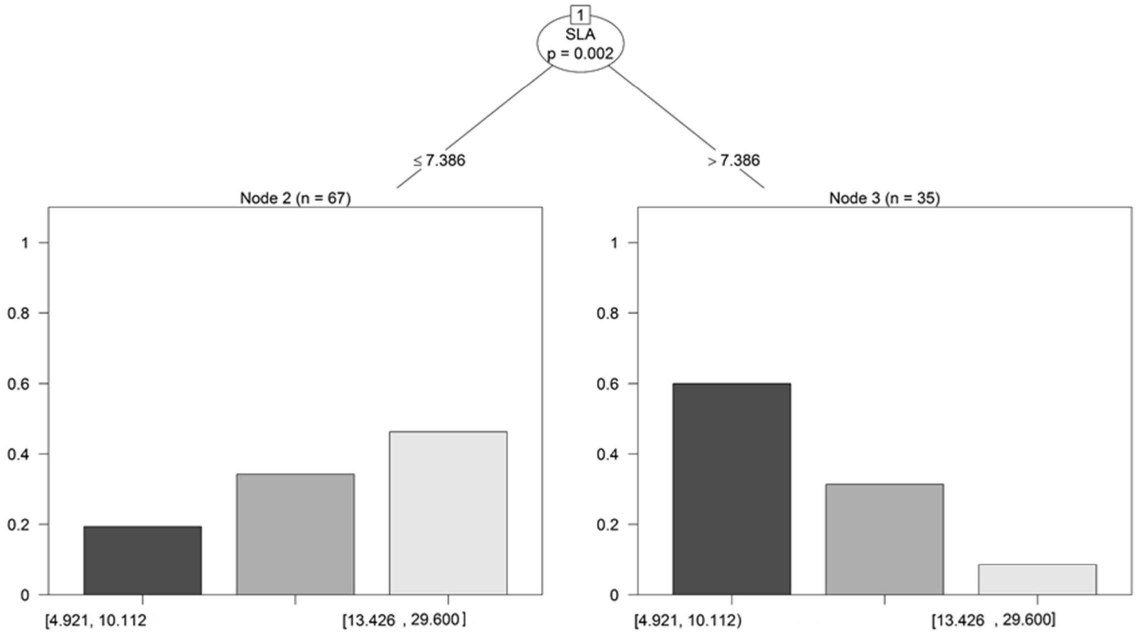

Fig. 8. Decision trees to classify plant species according to leaf SIRM grouped into three classes using quantile classification low (dark gray), medium (gray) and high (light gray) in September for (a) all considered plant species (b) deciduous broadleaf tree and shrub species (c) evergreen needle/scale-like, broadleaf, and climber species. The nodes in the decision tree represent plant species classification within the three leaf SIRM classes, and the branches of the nodes represent the decision rules or conditions.

Highlights

1. The leaves of 96 perennial plant species were investigated for differences in net particle accumulation.
2. Leaf surfaces with trichomes were more effective in net particle accumulation.
3. Leaf surfaces with reduced leaf wettability were less effective in net particle accumulation.
4. Leaves of the least and the most effective plant species were *Buddleja davidii* and *Populus alba* respectively.
5. The presence of trichomes and SLA were important leaf traits for classifying plant species in low, medium, and high net particle accumulators.

Declaration of interests

☒ The authors declare that they have no known competing financial interests or personal relationships that could have appeared to influence the work reported in this paper.

☐The authors declare the following financial interests/personal relationships which may be considered as potential competing interests: